

MASTER THESIS

# IMPROVEMENT OF OPENSIM MODEL FOR THE ESTIMATION OF LUMBAR TORQUES VIA EMG-DRIVEN MODELLING

Sanchana Krishnakumar

FACULTY OF ENGINEERING TECHNOLOGY  
DEPARTMENT OF BIOMECHANICAL ENGINEERING

EXAMINATION COMMITTEE

Dr. Ir. M. Sartori

Ir. A. Moya Esteban

Dr. Ir. B. J. F. van Beijnum

DOCUMENT NUMBER  
BE - 762

29-10-2020

UNIVERSITY OF TWENTE.



*“The only source of knowledge is experience, all the rest is information”*

- **Albert Einstein**



## **Preface**

Studying underlying principles of human movement mechanics has enabled scientists and engineers to create innovative solutions to assist, augment and empower human beings. Advancements in subject-specific musculoskeletal modelling techniques have greatly helped in achieving this goal. This paper is a result of my master thesis that aims to tackle the current limitations in studying the lumbar torques during lifting activities for industrial workers involved in manual material handling tasks.

This entire journey has been very challenging, and without the guidance of few people who always had my back and motivated me, I wouldn't have reached this far. Firstly, I would like to begin by thanking my Professor and chair Dr.Ir. Massimo Sartori for providing me with an opportunity to perform this master assignment in the Neuromechanical modelling and engineering lab at the University of Twente. I would also like to acknowledge his valuable comments during the progress meetings.

I would also like to extend my sincere gratitude to my daily supervisor Mr. Ir. Alejandro Moya Esteban for his constant support and encouragement throughout this research. His critical comments and feedback during the weekly meetings have certainly helped me to improve my research and scientific writing skills.

I would also like to acknowledge and extend my gratitude to Dr.Ir.Bert-Jan van Beijnum for agreeing to be part of my thesis graduation committee and for his valuable feedback on my report.

Last but not the least, my heartfelt thanks to my parents, family and friends for their constant love and support.

**Sanchana Krishnakumar**



# Contents

I.	INTRODUCTION .....	1
A.	Aim and scope of the project.....	2
II.	METHODS .....	2
A.	Subject and experimental setup .....	2
B.	Lifting tasks .....	3
C.	Experimental procedure.....	4
D.	Data pre-processing .....	4
E.	OpenSim musculoskeletal modelling and Data processing .....	5
F.	Improving the estimation of L5-S1 joint torques.....	5
1)	Modelling BOX kinetics (Only-Box model).....	5
G.	EMG driven modelling with CEINMS.....	5
H.	Statistical analysis .....	6
III.	RESULTS .....	7
A.	Symmetric lifting.....	7
B.	Comparison between both methods for symmetrical lifting tasks .....	7
C.	EMG driven modelling- CEINMS.....	8
D.	Asymmetrical Lifting .....	9
IV.	DISCUSSION .....	10
V.	CONCLUSION.....	12
	REFERENCES .....	12
	APPENDIX .....	14
A.	Conventions of OpenSim.....	14
B.	Creating Box model in Solidworks .....	14
C.	Adding the box to OpenSim model .....	15
1)	Box with a weld joint .....	15
2)	Box with a weld constraint.....	15
3)	Box with a free joint.....	16
D.	Symmetrical lifting tasks.....	16
E.	ANOVA for symmetric lifting tasks.....	17
F.	Asymmetrical Lifting tasks .....	18
	REFERENCES ( Appendix).....	19



## **List of Abbreviations**

**AL-** Asymmetric lifting tasks

**ANOVA-** Analysis of variance

**BSE-**Back support exoskeletons

**CEINMS-** Calibrated EMG-informed neuromusculoskeletal modelling toolbox

**DOF-** Degrees of freedom

**EMG-** Electromyography

**GRF** – Ground reaction force

**ID-** Inverse dynamics

**IK-**Inverse kinematics

**LFB-** Lifting full body model

**LT-** lift and transfer task

**MOtoNMS-** Matlab motion data elaboration toolbox for neuromusculoskeletal applications toolbox

**MTU-** Musculotendon unit

**RMSE-** Root mean square error

**sEMG-** Surface electromyography

**SL-**Symmetric lifting tasks

**TT-** Twist and transfer task



# Improvement of OpenSim model for the estimation of lumbar torques via EMG-driven modelling

Sanchana Krishnakumar<sup>1</sup>, Alejandro Moya Esteban<sup>1</sup>, Massimo Sartori<sup>1</sup>, Bert-Jan van Beijnum<sup>2</sup>

<sup>1</sup> Department of Biomechanical Engineering, University of Twente, 7522NB Enschede, The Netherlands

<sup>2</sup> Department of Biomedical signals and systems, University of Twente, 7522NB Enschede, The Netherlands

**Abstract:** Lower-back problems are one of the major causes of work-related injuries in manual material handling industries. Back support exoskeletons (BSE) are used to aid workers during manual handling activities. EMG controlled BSE utilize surface electromyography to control the exoskeleton. Control strategies of these BSE can be realized by understanding the underlying user movement mechanics with help of musculoskeletal modelling. Most full-body models in OpenSim do not include the object that is being lifted therefore making it difficult to account for external hand forces during lifting tasks. **Objective:** This paper aims to develop a method to account for accelerations and rotational torques from the external object to improve modelling. **Methods:** We proposed an indirect methodology to include external hand forces during inverse dynamics (ID) computations in OpenSim. The proposed methodology was tested for both symmetric and asymmetric box lifting tasks for 3 weight conditions (1.2, 6.2, 16.2kg) and L5-S1 torques were estimated using ID and EMG-driven modelling approaches. **Results:** The new methodology improved L5-S1 peak ID torque estimates and the largest increase was 23.8Nm for 16.2kg. ANOVA indicated significant differences between peak torque estimates between both methods ( $p < 0.05$ ). The resulting ID torques were used to calibrate the EMG driven model (CEINMS). CEINMS torques were also compared against the respective L5-S1 ID torques. Results indicated a good correlation ( $r^2 > 0.89$ ) and low RMSE (5.97-21Nm) between both ID and CEINMS estimates. The proposed methodology represents a valid approach to include external object forces to estimate realistic L5S1 joint torques during lifting activities via ID and EMG driven modelling approaches.

**Index terms:** Back support exoskeletons, EMG-driven modelling, Inverse dynamics (ID), Lumbar torques, subject-specific musculoskeletal modelling.

## I. INTRODUCTION

Lower back disorders are identified as one of the major work-related musculoskeletal disorders (MSDs) and account for roughly 40% of the total work-related MSDs [1]. Studies suggest that the prevalence of lower back disorders is higher in industries that involve manual material handling tasks such as heavy load lifting, and prolonged stoop or bent postures [1, 2, 3, 4]. The load at the lower back is usually studied around the lumbo-sacral (L5-S1 joint) [5, 6, 7]. Various biomechanical studies have proved that manual handling of heavy loads increases spinal compressive forces up to 5000N and increases the

risk of lower back disorders or injuries [2, 4, 8, 9]. These injuries not only increase the economic burden of companies but also affects the quality of life of the workers [2, 4].

Many attempts have been made to reduce spinal forces and aid workers during manual handling activities such as recommending biomechanically safe lifting techniques, limiting the time of exposure and automating the activities [10, 11]. However, these solutions are not feasible in scenarios with limited spaces and reduce flexibility of the tasks that are being carried out [11]. In such scenarios, an external aid or use of an exoskeleton to generate forces or torques to support the workers could be employed [8].

Exoskeletons are wearable devices that help augment human power and assists in performing physical activities by applying forces or torques to one or multiple joints of the body [2, 8, 11]. The use of exoskeletons for occupational use has been increased over recent years. They are now being used in multiple industries such as logistics, automotive, steel, agricultural and for military activities [12, 13, 14, 15]. The primary goal of an exoskeleton used in industries is to provide support without restricting the movements of the workers and to reduce the risk of MSDs [16]. Based on the type of actuation mechanism used to provide support, the exoskeletons can be classified into active or passive. Passive exoskeletons do not comprise of any actuators but use materials like spring and dampers that store the energy of the user and release it when needed to provide support [17, 18, 19, 20]. Active exoskeletons use one or more actuators to support the user in producing torques or forces. These actuators could be electric, hydraulic, pneumatic [4, 8, 9, 21].

Active exoskeletons can further be classified based on their control methods into direct and indirect control. Indirect control depends on measurement of joint angles and loads applied on the body measured from the device or the environment. This can be achieved with the help of inertial measurement sensors. These sensors can be used to obtain joint angles and 3D orientations of body segments. This information could then be used to achieve the required control [2]. The direct control approach is based on the bio-signals acquired from the user such as surface electromyography (sEMG) that are measured from target muscle groups. The muscle activations measured from the sEMG can be used for controlling the exoskeleton after post-processing [22, 23].

To design efficient control strategies and to study the biomechanical effects of back exoskeletons, it is critical to study and understand the underlying user movement dynamics, and lumbar forces. Generally, lumbar compressive forces are measured either by invasive intradisc pressure measurements or by instrumented vertebral body replacement systems (VBR) [24]. However, utilizing these systems in real-time for control of exoskeletons is not feasible because of their invasive nature. These joint compressive loads can also be indirectly measured with help of subject-specific musculoskeletal modelling techniques [25]. Utilizing a musculoskeletal model for dynamic simulations can be advantageous to account for forces from muscles which cannot be measured directly [26,27].

Subject-specific musculoskeletal modelling has been widely used to study joint kinematics and torques during dynamic activities [28]. Platforms like OpenSim and Anybody allow musculoskeletal modelling with either forward dynamics or Inverse dynamics (ID) approaches [29, 30]. Lifting tasks can be studied in OpenSim (SimTK, Stanford, CA) by using open source generic models specifically designed for lifting activities. Inverse kinematics (IK) and ID with OpenSim can help in studying the joint kinematics and torques during lifting activities [6, 31].

EMG driven musculoskeletal modelling approach, on the other hand, is a forward dynamic modelling approach that can estimate internal body properties such as joint torques, muscle forces, or lumbar compressive forces by utilizing non-invasive EMG recordings [32]. Several EMG driven models with different complexities have been used to compute lumbar torques and are reported by Lloyd et al. in [33].

Calibrated EMG-Informed Neuromusculo-skeletal modelling (CEINMS toolbox) is an OpenSim plugin to implement previously tested and validated EMG-driven algorithms. CEINMS has been tested to work with a wide range of OpenSim models consisting of any number of musculotendon units (MTU) and multiple DOF models [33, 34]. Typically, torques from EMG-driven models are validated against the torques obtained by the ID approach [33]. Although CEINMS has been previously validated for a wide range of tasks including gait, it has not yet been validated for lifting tasks.

EMG driven modelling in CEINMS requires an offline calibration procedure to build subject-specific models calibrated for parameters such as activation dynamics, tendon slack length, optimal fiber length and strength coefficient of the muscles. The parameters required for calibration include reference ID joint torques, MTU length and muscle moment arms. Once calibrated, the EMG-driven model can estimate the MTU forces and joint torques based on input EMG signals and joint angles [35].

Typically these calibration parameters for lifting tasks can be obtained by inverse dynamics and muscle analysis

computations with currently available full-body musculoskeletal models. Although OpenSim has a large library of full-body models, none of the existing full-body models for lifting tasks includes the external object that is being lifted. Due to these limitations, researchers have to compute the external hand forces for ID computations. Moya-Esteban et al. [36] assumed forces from the object being lifted to be equal to its weight due to gravity. This assumption poses limitations as it is not valid during dynamic lifting tasks. Based on this assumption, the rotational torques and forces due to accelerations of the object acting on the hands are not accounted for during ID computations. Therefore, this assumption does not provide a realistic modelling condition and needs improvement.

Balche et al. studied one-handed lifting tasks by adding an object that is being lifted to the generic OpenSim shoulder model and validated it for overhead lifting tasks [37]. However, the model only included shoulder and cannot be used to study lumbar torques. Gauvreau et al. studied different methods to include hand forces from the object (box) for lifting tasks during ID computations. Changing the mass of the hands based on the mass of the object, produced better L5-S1 torque estimates [38]. However, this technique does not also account for the inertial properties of the object being lifted. Since the external hand forces are not correctly estimated, this may result in improper calibrations of the EMG-driven models to predict the L5-S1 torques during lifting activities.

#### A. Aim and scope of the project

Considering the lack of validation studies of the CEINMS toolbox for different lifting tasks and the lack of OpenSim full-body lifting models with integrated external objects. There is a need to account for hand forces and torques from the object to study lifting tasks. Therefore, this project aims to

- i. Propose and implement a new methodology to account for rotational torques and forces due to accelerations of the box for both symmetric and asymmetric lifting tasks.
- ii. Estimate L5-S1 torques using EMG driven musculoskeletal modelling via CEINMS and validate CEINMS toolbox for lifting tasks by comparing the resulting torques against ID torques from OpenSim.

Due to limited time frame, although joint compressive loads for both symmetric and asymmetric lifting tasks can be estimated through OpenSim with knowledge of muscles forces estimated through CEINMS, this project aims to validate CEINMS toolbox only till a torque level for symmetric lifting tasks.

## II. METHODS

#### A. Subject and experimental setup

A healthy male volunteer (age:26, weight:70kg and height:1.75m) with no history of back pain was recruited for this study.

A box with dimensions 40 cm x 30 cm x 22 cm (width x depth x height) and weighing 1.2 kg was filled with different weights to simulate different weight conditions (1.2,6.2,16.2 kg). Sixty spherical reflective markers (36 anatomical and 24 cluster markers) were placed on the body of the subject with double-sided adhesive tape to determine subject kinematics. The placement and description of the markers can be seen in **Fig 1** and **Table I** respectively.

TABLE I

## SEGMENT-WISE DESCRIPTION OF MARKER PLACEMENT

Segment	Name of the marker	Placement
Trunk	RACR/LACR	Acromion
	CLAV	Clavicular notch
	STER	Mid sternum
	C7	7 <sup>th</sup> cervical vertebra
	T10	10 <sup>th</sup> thoracic vertebra
Arm	RUA/LUA(1,2,3)*	Mid-lateral upper arm
	RLHE/LLHE	Lateral epicondyle on the humerus
	RMHE/LMHE	Medial epicondyle on the humerus
	RF/LF(1,2,3)*	Mid-lateral forearm
	RUS/LUS	Styloid process (ulna)
	RRS/LRS	Styloid process (radius)
	R2K/L2K	2 <sup>nd</sup> Metacarpophalangeal joint
	R5K/L5K	5 <sup>th</sup> Metacarpophalangeal joint
Pelvis	RASI/LASI	Anterior superior iliac spine
	RPSI/LPSI	Posterior superior iliac spine
Leg	RT/LT(1,2,3)*	Mid-lateral thigh
	RLF/LLFE	Lateral epicondyle on the femur
	RMFE/LMFE	Medial epicondyle on the femur
	RS/LS(1,2,3)*	Mid-lateral shank
	RCAL/LCAL	Calcaneus
	RLM/LLM	Lateral cunifform
	RMM/LMM	Medial cunifform
	R2MT/L2MT	2 <sup>nd</sup> Metatarsophalangeal joint
	R5MT/L5MT	5 <sup>th</sup> Metatarsophalangeal joint

**Note:** R<sub>xx</sub>/L<sub>xx</sub> represents the marker placed at the same anatomical position both on the left and right side of the body.

\* represents cluster triads RX(1,2,3) represents RX1, RX2 and RX3

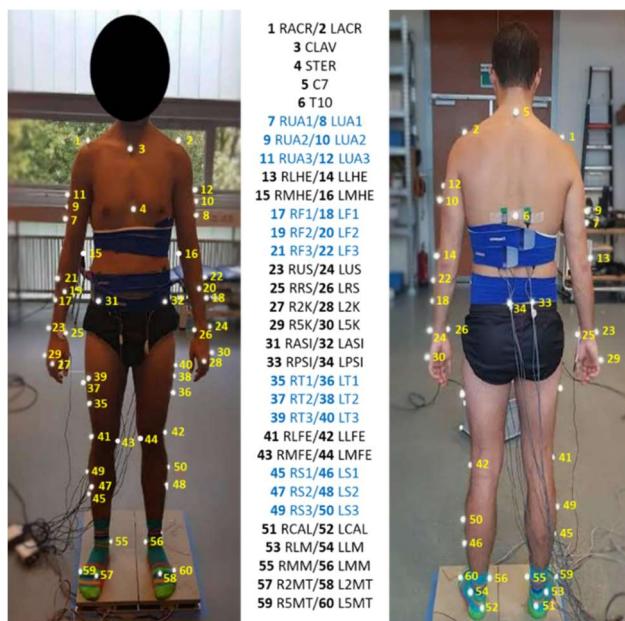


**Fig 1.** The figure depicts the marker placement on the volunteer. Anatomical markers on bony landmark marks are presented in black colour while the cluster markers are represented by blue colour.

Eight markers were also used to identify the corners of the box that was being lifted. Qualisys motion capture system

(Qualisys Medical AB, Gothenburg, Sweden) was used to record the experimental sessions. The 3D marker trajectories of the subject, as well as the box, were tracked using 10- Oqus camera system from Qualisys at a frame rate of 128 Hz. Ground reaction forces (GRF) and moments were measured using a portable dual force plate (AMTI, MA, USA) at 2048 Hz.

EMG system from Delsys (Delsys Bagnoli, Delsys, Boston, MA) was used to record EMG signals at a sampling rate of 2048Hz. 12 bipolar electrodes were placed bilaterally to record the six muscle groups that are active during lifting and lowering activities. Electrodes were placed as described in Kingma et al. [39]. An overview of EMG placement and muscles that were recorded can be seen in **Table II**. The reference electrode was placed at the pisiform bone on the right wrist. All the measured signals, as well as the marker trajectories, were synchronized by Qualisys track manager software.

TABLE II  
EMG ELECTRODE PLACEMENT FOR BOTH LEFT AND RIGHT MUSCLES

Electrode	Muscle	Placement
1/2	Rectus abdominis	Level of umbilicus
3/4	Internal oblique	Superior to the inguinal ligament
5/6	External oblique	Placed between the iliac crest and lowest edge of the ribcage
7/8	Iliocostalis lumborum	6 cm from the spine at the L2 level
9/10	Longissimus thoracis pars lumborum	3cm from the spine at the L1 level
11/12	Longissimus pars thoracis	4cm from the spine at the T10 level

**Note:** 1/2 represents right and the left electrode respectively

### B. Lifting tasks

Symmetric lifting and asymmetric lifting (SL and AL) box lifting tasks were studied in this research. For each of these lifting tasks, two different box lifting actions were studied. The tasks are reported in **Table III**.

TABLE III  
OVERVIEW OF LIFTING TASKS AND ACTIONS

Lifting Tasks	Actions/techniques
Symmetric	Squat lifting
	Stoop lifting
Asymmetric	Lift and transfer
	Twist and transfer

SL involved lifting a box placed in front of the subject in mid-sagittal plane with either squatting (bending down with knees flexed and keeping the trunk as upright as possible) or stooping (bending the torso with extended knees) techniques as seen in **Fig 2**. The box was placed on the ground level and the subject was free to choose the horizontal distance between the feet and the box. AL involved two different lifting patterns: lift and transfer

(LT) and twist and transfer (TT). During LT, the subject adopted a free lifting technique to pick up the box placed in the midsagittal plane on the ground and transferred the box to a table placed at 60 degrees towards the right of the subject. This was followed by coming back to the standing position as seen in **Fig 2**. The second asymmetrical lifting technique was TT. One repetition of TT involved two twist and transfer movements. The first was to lift the box placed at 60 degrees to the mid-sagittal plane to the left of the subject at a height of 41cm. This was followed by transferring the box to another table at the same height and placed 60 degrees to the right. After transferring, the subject came back to the standing position. The second transfer movement involved lifting the box from the table on the right and placing it back on the left table before coming back to the original standing position as seen in **Fig 2**.

### C. Experimental procedure

The subject performed each lifting method (SL and AL) in two different experimental sessions. Before beginning each experimental session, the electrode application area was shaved and cleaned with alcohol. EMG electrodes and markers were attached using double-sided adhesive tapes based on the placement locations as described in **Table I** and **Fig 1**. Maximum voluntary contraction (MVC) measurements were recorded for the abdominal and trunk muscles by asking the volunteer to counteract a strong thrust applied against them from a supine and prone position, respectively. Consequently, to scale the OpenSim generic model, a static trial with no subject movement was recorded.

All the lifting trials were performed by the volunteer standing on the force plate and lasted for 20 seconds. Each symmetric trial involved 2 repetitions of either squat or stoop lifting. During the first experimental session, a total of 6 trials were recorded for each experimental weight and lifting condition and resulted in a total of 12 repetitions for each experimental condition. Sufficient rest was given in between the trials to minimize muscle fatigue. One repetition of squat and stoop lifting is explained in **Fig 2**.

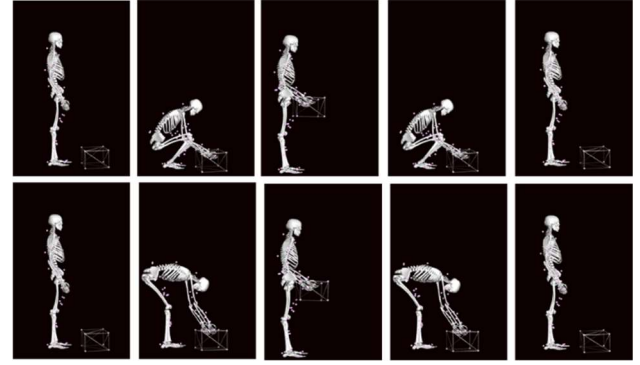


**Fig 2. Squat lifting (1<sup>st</sup> row):** Squat lifting involves squatting down from an upright position to lift the box and moving back to the upright position with the box. This is followed by squatting with the box and placing it back on the ground before going back to the upright position. **Stoop lifting (2<sup>nd</sup> row)** Stoop lifting involves bending down from an upright position to lift the box and moving back to the upright position with the box. This is followed by bending down with the box and placing it back on the ground before going back to the upright position.

One trial of LT and TT involved 2 repetitions of lifting and transfer task and twist and transfer, respectively. During the second experimental session, a total of 4 trials were recorded for each experimental weight and asymmetric lifting condition. This resulted in a total of 8 repetitions per experimental condition. One repetition of LT and TT is explained in **Fig 3**.

### D. Data pre-processing

The MOtoNMS (Matlab Motion data elaboration toolbox for neuromusculo-skeletal applications) toolbox for MATLAB by Mantoan et al.[40] was used to pre-process the data and get inputs for OpenSim and CEINMS. Data from Qualisys system consisting of raw 3D marker coordinates, GRF as well as the EMG data was given as input to the MOtoNMS tool. The processing pipeline of the tool along with the processing pipeline for OpenSim is represented in **Fig 5**. The MOtoNMS tool filters marker trajectories, GRF forces and moments with a zero-lag 2<sup>nd</sup> order low pass Butterworth filter with a cut-off frequency of 6 Hz. EMG signals were processed by removing the mean of the signals followed by a zero-lag band-pass filter with a cut off frequency of 30, 300 Hz.

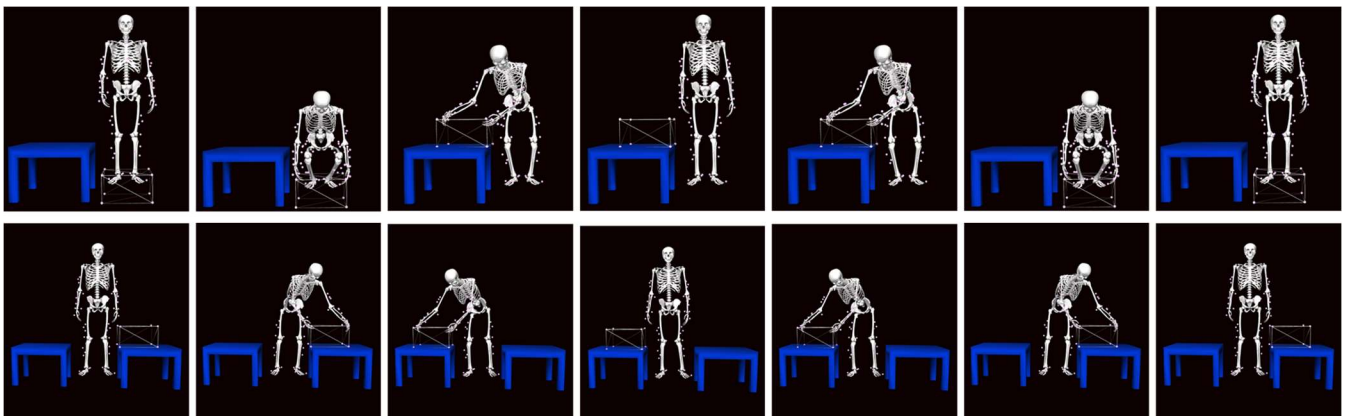


**Fig 3. Lift and transfer (1<sup>st</sup> row):** Lift and transfer involves free lifting of the box and placing the box on the table toward the right before coming to the original position. This is followed by picking up the box again and placing it back on the ground before going back to the upright position. **Twist and transfer (2<sup>nd</sup> row)** Twist and transfer involve transferring the box from one table to another table before going back to an upright position. This is followed by transferring the box back to the original position.

The filtered signals were then full-wave rectified and filtered with a low pass filter with a cut off frequency of 6Hz to produce EMG linear envelopes [33]. The EMG signals recorded during the MVC trials were used to find the maximum muscle activations and successively normalize the EMG signals for the trunk muscles recorded during lifting trials [40]. The resulting EMG envelopes will be used for EMG-driven modelling as represented in **Fig 5**.

The MOtoNMS toolbox was adapted to include the hand forces exerted by the box during dynamic lifting tasks. For squat and stoop lifting, the base marker coordinates of the box were used to identify the position. The box was considered to be in motion when all the 4 base markers were at least 1cm above the ground. The identified time instances were used to apply the force to the hands. To apply hand forces for AL tasks, the velocity of the base markers was used to identify the lifting instances. The hand forces were applied during the time instances at which the velocity was not zero. The hand forces were computed by multiplying the weight of the box with the gravity component. The load was assumed to be equally distributed between both the hands.

#### *E. OpenSim musculoskeletal modelling and Data processing*

The OpenSim lifting full-body model (LFB) designed by Gauvreau et al. was used to study lifting tasks in this study [31]. The LFB model consists of 30 rigid body segments with 29 degrees of freedom (DOF) and 238 MTU units. The generic LFB model was scaled to match the anthropometric properties of the volunteer using the scale toolbox in OpenSim. The scaling factors were computed using the anatomical marker positions recorded during the static trial. The scaled model was used for further computations. IK was performed to obtain joint angles at each time frame using IK toolbox of OpenSim using 3D marker positions. All markers except elbow and knee (RMHE, RLHE, RLFE, RMFE, LMHE, LLHE, LLFE, LMFE) were used for IK computations. ID was performed to compute L5-S1 joint torques. Hand forces along with ground reaction forces and moments were given as external forces during the ID computation. Hand forces were applied to the midpoint between the 2<sup>nd</sup> and the 5<sup>th</sup> metacarpophalangeal joints of both the hands. GRF forces and torques were applied at the calcaneus of the respective legs. The resulting L5-S1 torques from this method will be considered as the baseline torques. The estimates from other methods will be compared against the torques from this method. Muscle analysis was performed using the “Analyze” tool of the OpenSim to obtain MTU lengths and moment arms for the L5-S1 flexion-extension coordinate for symmetric lifting. All the trials were batch-processed (IK, ID and MA) using the BOPS toolbox (Batch OpenSim Processing Scripts) for OpenSim. L5-S1 torques obtained from ID method will hereafter be referred to as L5-S1 torques from the old method. The process pipeline can be seen in **Fig 5**.

#### *F. Improving the estimation of L5-S1 joint torques*

To improve the estimation of the L5-S1 joint torques, rotational and vertical accelerations of the box have to be accounted for. A model of the box described in section X was designed with OpenSim’s coordinate convention in SolidWorks (Dassault Systems, Vélizy-Villacoublay, France). Individual models were created for respective weight conditions (1.2 kg, 6.2kg and 16.2kg) and dimensions 40 cm x 30 cm x 22 cm (width x depth x height) . Two different designs were created for each weight condition, one with the origin frame defined at the center of mass of the box and the other with the origin defined at the center of the base. The inertial properties as well as the definitions of mass properties of each design along with the export settings is reported in **Appendix B**. The models were then exported from SolidWorks.

Several approaches were tested to include the box as an additional body into the LFB model (by defining different joints and constraints such as weld joint, weld constraints and free joint). These approaches are explained in **Appendix C**. All of these methods could not be successfully implemented or could not accurately model the forces and torques resulting from the box. They are discussed in detail in the discussion section. The approach of modelling the box as an individual object was chosen to compute the kinetics of the box.

##### *1) Modelling BOX kinetics (Only-Box model)*

The box was created as an individual OpenSim model with just one body and a free joint with the ground. Separate models were created for different weight conditions and the origin of the box was considered to be at its centre of mass. The mass and inertial properties for each weight condition were defined in respective OpenSim model. IK and ID computations were performed. The ID computation resulted in 3 translational forces and three rotational moments of the box (will be referred to as only-box ID). IK for the LFB model without the box was performed and the forces derived from the only-box ID computation were used to define the external loads during the ID computations for the LFB model. The L5-S1 torques obtained from this method will hereafter be referred to as L5-S1 torques from the new method.

#### *G. EMG driven modelling with CEINMS*

L5-S1 joint torques were also estimated via EMG-driven modelling. Muscle forces, muscle activations and L5-S1 torques were estimated from the EMG recordings. The estimation involved two steps namely calibration and execution. The process is depicted in **Fig 4**. The calibration step was required to adapt the uncalibrated model obtained from OpenSim to match the anatomical and physiological parameters of the subject. Calibration step involved determining subject-specific model parameters by calibrating with a set of nominal parameters such as MTU length, moment arms, ID joint torques from OpenSim and EMG recordings measured during the experiment trials [35]. The calibration and the execution step involved an additional setup file to map the recorded EMG signals to

the muscles of the OpenSim musculoskeletal model. The calibration step was followed by the execution step as seen in Fig 4. The CEINMS block presented in Fig 5 is elaborated and illustrated in Fig 4. The executions were performed for unique trials that were previously not used for calibration of the model. During execution, MTU forces and L5-S1 joint torques were predicted as a function of the input EMG signal recordings and joint angles.

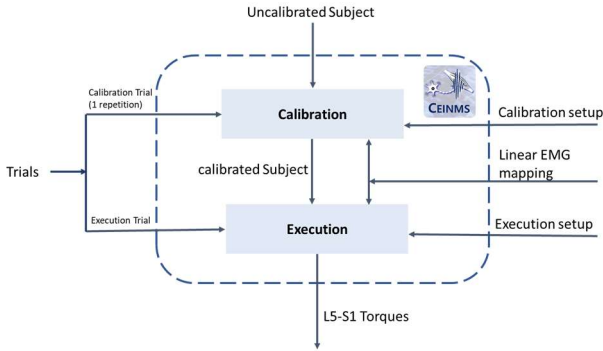


**Fig 4.** Schematic illustration of EMG driven modelling process was adapted from figure 1 in Pizzolato et al. [34]. The uncalibrated subject file is used as initial input for calibration. The muscle parameters in the uncalibrated subject file are calibrated with help of the calibration setup and trials provided. The calibration setup defines the type of calibration and assumptions. The EMG mapping defines the neural mapping of the measured EMG signals to the muscles in the subject file or assigns it with a zero EMG (passive muscle). The calibrated subject file is given as an output from calibration and is used to predict muscle activations, forces and torques for input trials. Execution setup defines the type of neural algorithms to be implemented. A predictive open-loop neural algorithm was used in this research.

To compare the performance of the EMG-driven model based on the trials used for calibration as well as to validate the EMG-driven model for lifting tasks, multiple models were calibrated with varying input parameters. The

calibration trials used to obtain the calibrated models are reported in Table IV. Two versions of calibrated models were obtained by calibrating with ID torques obtained with old and new method in OpenSim. The L5-S1 joint torques estimated by the calibrated models were then validated against their respective reference ID torques (Old and new).

TABLE IV  
WEIGHT CONDITIONS USED FOR CALIBRATING THE CINEMIS MODEL

Calibrated model	Trials used for calibration
Squat lifting	One repetition from the squat lifting of all three weight conditions (1.2,6.2,16.2kg)
Stoop lifting	One repetition from stoop lifting of all three weight conditions (1.2,6.2,16.2kg)

#### H. Statistical analysis

Peak torques were calculated for all the trials and experimental conditions. RMS and  $r^2$  values were computed between the averaged torques obtained from old and new ID torques for respective weight conditions. To test if the estimates between both the methods were statistically significant, an ANOVA was applied. The data passed Shapiro-Wilk normality test and met all the assumptions of a generalized linear model ANOVA. The estimation method, lifting technique and weight condition were considered to be independent factors. The effects of the interaction of the independent factors were also studied. Error differences between old and the new torques for each repetition were calculated.

RMS values and  $r^2$  values were studied between L5-S1 CEINMS torques and the respective reference ID L5-S1 torques.

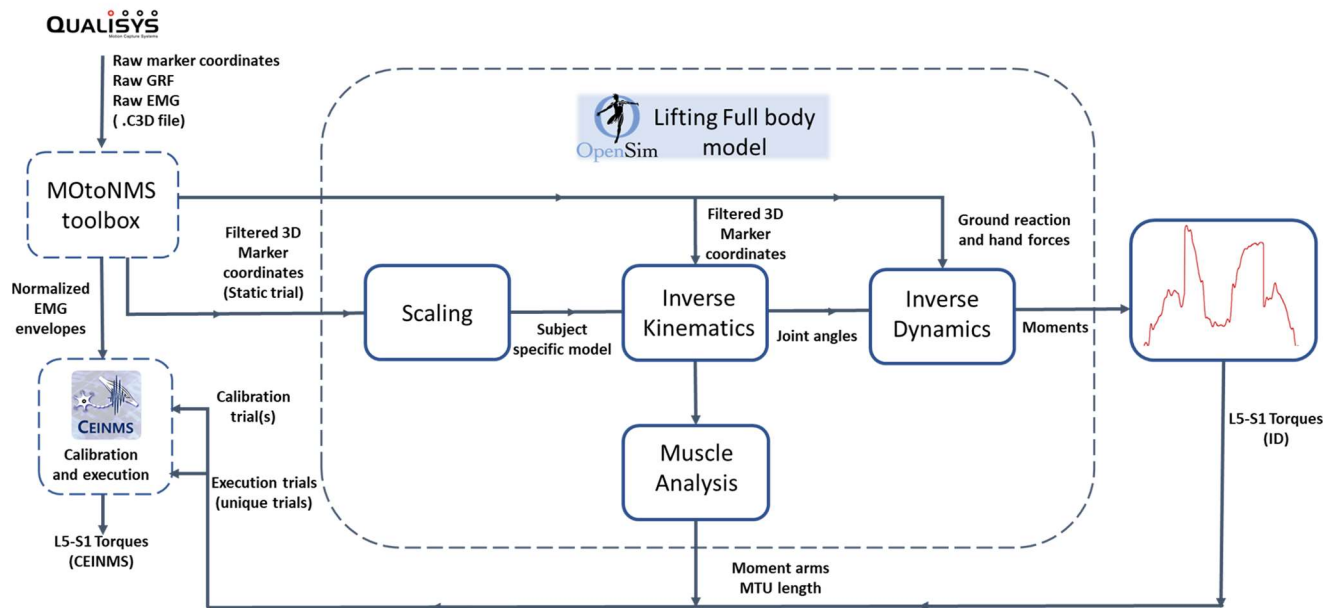


**Fig 5.** Overview of the data processing pipeline explained in subsections 2.D-2.F. The measured signals are given as input to the MOtoNMS toolbox. The files are elaborated to give filtered marker coordinates, forces and normalized EMG envelopes as output. The filtered marker coordinates and the forces are used as input for OpenSim processing while the normalized EMG envelopes are used for EMG driven modelling (CEINMS). The L5-S1 ID torques from OpenSim processing are considered as baseline torques and are used to calibrate the EMG-driven modelling along with the MTU length and moment arm from muscle analysis toolbox in OpenSim. Unique trials not used for calibrations are given as execution trials to estimate CEINMS torques. → Represents inputs and outputs while --- represents toolbox or processing software blocks.

### III. RESULTS

Comparisons between L5-S1 torque estimates from OpenSim with both old and new methods (constant hand force vs hand force based on box forces and torques respectively) are shown here. L5-S1 torques estimated via EMG-driven modelling with CEINMS are also presented in this section.

#### A. Symmetric lifting

For all symmetric lifting trials, L5-S1 flexion-extension (F-E) ID torques estimated with the old method and the new method can be seen in **Fig 6**. At 0% of the lifting cycle, the subject remained in the upright posture and this resulted in torque of approximately 0 Nm as there was minimal flexion or extension. 0-20% of the cycle corresponds to the time interval at which the subject bent forward to pick up the box and thus resulted in an increase in torque. The sudden torque increase observed around 20% of the cycle corresponds to the instance of picking up the box from the ground. This is clear in 6.2 and 16.2 kg conditions. The highest L5-S1 torques (F-E) were observed between 20% and 30% of the lifting cycle, which corresponds to the time interval at which the subject lifted the box from the ground (lift off) to come back to the upright position. The peak torque around 30% will be described as the L5-S1 peak torque. 30-50% of the lifting

cycle represents the interval at which the subject moved back to the upright position while carrying the box. The second part of the cycle is the lowering task represented between 50-70% of the cycle, where the subject moved to drop the box to its original position on the ground (drop off). This was followed by going back to the upright position without the box (80-100% of cycle) and thus the L5-S1 (F-E) torque decreases and goes back to 0 Nm when the subject is completely back to the upright position. One repetition of both squat and stoop lifting is explained with figures in **Appendix D**.

L5-S1 (F-E) peak torques can be seen to increase with the increase in weight of the box being lifted in **Fig 6**. The peak torques for squat lifting and stoop lifting tasks are reported in **Table V**. The highest peak torque was estimated for stoop lifting technique with highest weight condition (16.2kg).

#### B. Comparison between both methods for symmetrical lifting tasks

The average L5-S1 ID torques with new and old method are presented in **Fig 6**. Values of peak lifting torques observed at 30% for all the trials were averaged and are represented along with peak torque differences between both the methods in **Table V**.

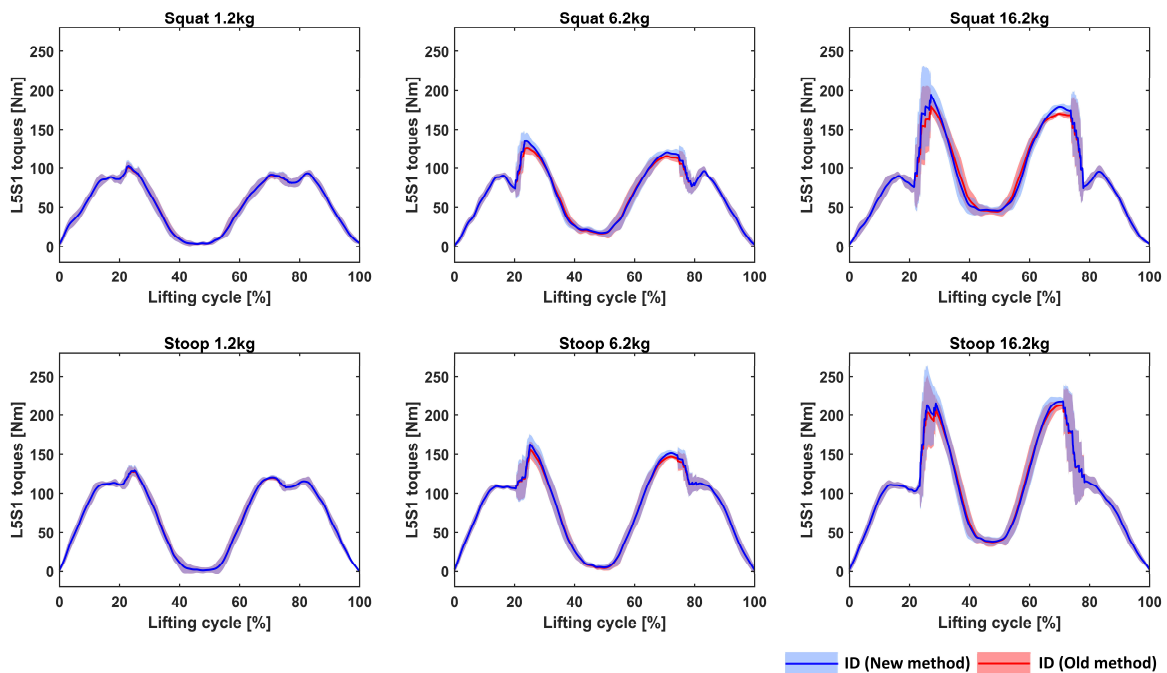


**Fig 6.** Comparison between L5S1 (F-E) ID torque estimates with both methods (old and new). Solid lines represent the average torques across repetitions and shaded areas correspond to  $\pm 1$  standard deviation.

TABLE V  
AVERAGE L5-S1 PEAK TORQUES FOR SYMMETRIC LIFTING. STANDARD DEVIATIONS ARE SHOWN IN PARENTHESES

Lifting condition	New method (1) peak torque	Old method (2) peak torque	Difference (1-2) (Nm)	RMS (Nm)	r <sup>2</sup>
Squat 1.2kg	117.60(4.80)	114.90(4.40)	2.70	0.34	1.00
Squat 6.2kg	151.90(8.10)	138.60(6.70)	13.30	2.50	1.00
Squat 16.2kg	219.90(8.90)	195.20(6.60)	23.80	5.12	0.98
Stoop 1.2kg	142.00(4.70)	140.30(4.40)	2.30	0.33	1.00
Stoop 6.2kg	178.20(4.50)	168.20(3.39)	10.00	1.75	0.99
Stoop16.2kg	248.90(7.40)	230.70(3.76)	18.20	2.75	0.99

The new method resulted in an increase of L5-S1 peak torque estimates for all the lifting tasks across all repetitions. The highest difference was observed for squat 16.2kg condition as seen in **Table V**. The RMS and  $r^2$  were computed for the mean L5-S1 torques for the entire 100% of the trial (see **Table V**). Torques from both the estimation methods resulted in similar curves and high  $r^2$  values ( $>0.98$ ) for all the trails. For both squat and stoop lifting technique, the weight condition of 16.2kg resulted in the highest RMS. Histogram differences between peak torque estimates for all the individual trials are shown in **Fig 7**.

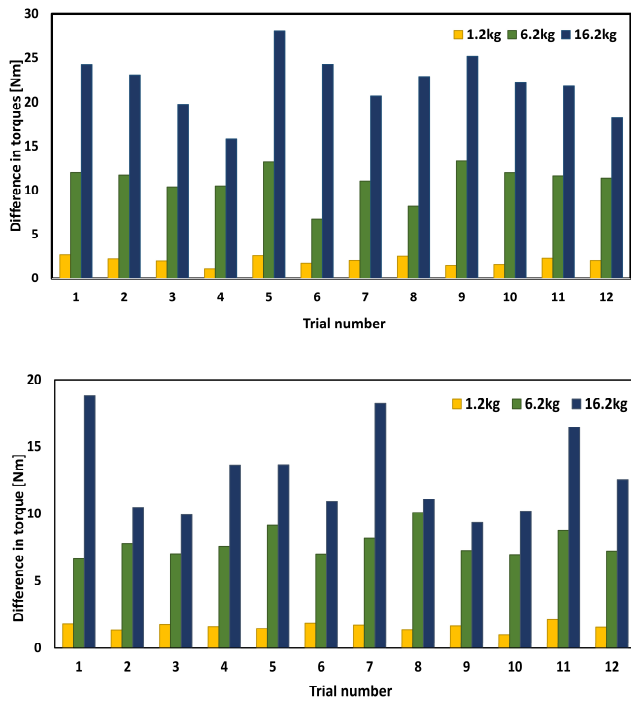


**Fig 7.** Difference between ID L5-S1 torques estimations between new method and old method a. Squat lifting b. Stoop lifting

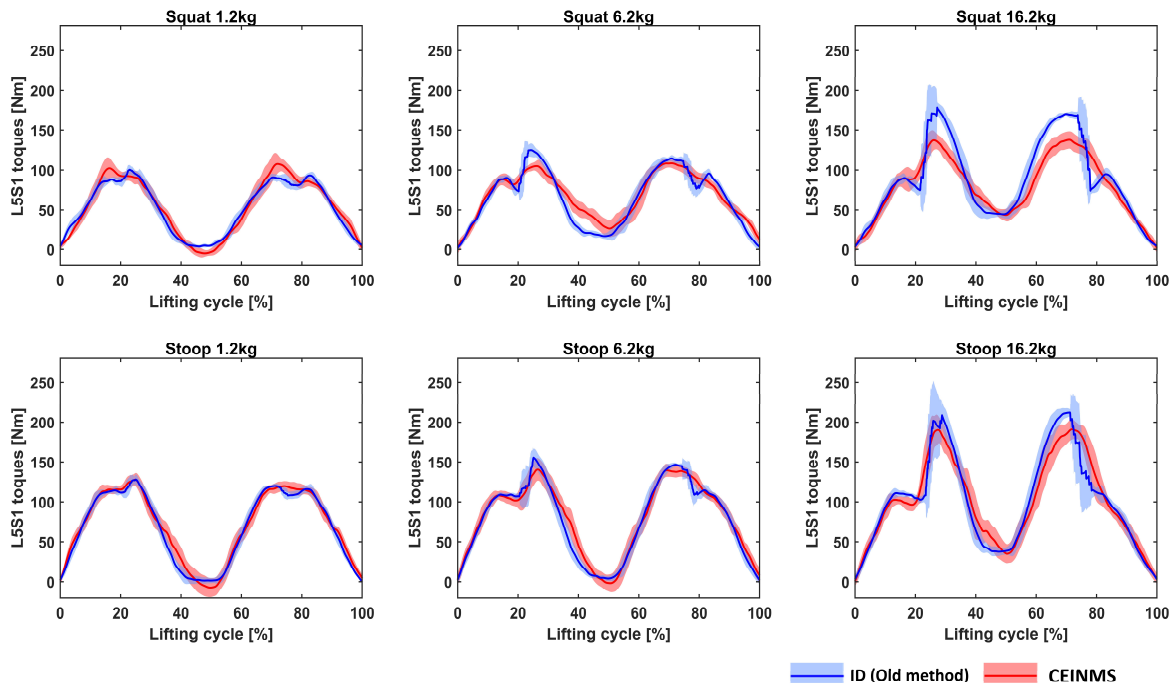


**Fig 8.** L5S1 torque estimates with OpenSim old method and CEINMS. Solid lines represent the average torques across repetitions and shaded areas correspond to  $\pm 1$  standard deviation.

ANOVA indicated significant differences in peak torque estimates between the two estimation methods (old and new) with  $p < 0.05$ . Significant differences between both the methods with  $p < 0.05$  was also observed for independent variables such as lifting methods and weight. Interactions between weight and the lifting method were also proved to be significant with  $p < 0.05$  for the L5-S1 torques. The results of ANOVA are reported in **Appendix E**.

### C. EMG driven modelling- CEINMS

**Fig 8** represents the comparison between the L5-S1(F-E) ID torques obtained with the old method and L5-S1(F-E) torques predicted by CEINMS models that were calibrated for squat and stoop lifting individually with all the weight conditions (1.2,6.2,16.2 kg). CEINMS torques from model calibrated with the new ID torques indicated good correlation with the reference ID torques ( $>0.90$ ) for all the lifting conditions. The highest correlation and lowest RMSE were observed for 1.2 kg weight condition for both squat and stoop lifting. The RMSE and  $r^2$  values for all the lifting conditions are reported in **Table VI**. Highest weight condition (16.2kg) resulted in largest RMSE for both squat and stoop respectively.

TABLE VI  
 $R^2$  AND RMSE VALUES FOR L5S1 TORQUES BETWEEN OLD ID AND CEINMS, NEW ID AND CEINMS.

	Squat 1.2 kg	Squat 6.2 kg	Squat 16.2 kg	Stoop 1.2 kg	Stoop 6.2 kg	Stoop 16.2 kg
ID torque with old method and CEINMS						
$r^2$	0.95	0.92	0.9	0.98	0.97	0.93
RMSE	7.6	11.21	19.69	6.47	8.42	15.26
ID torque with new method and CEINMS						
$r^2$	0.96	0.9	0.89	0.98	0.97	0.91
RMSE	7.8	12.03	21.85	5.98	8.16	17.30

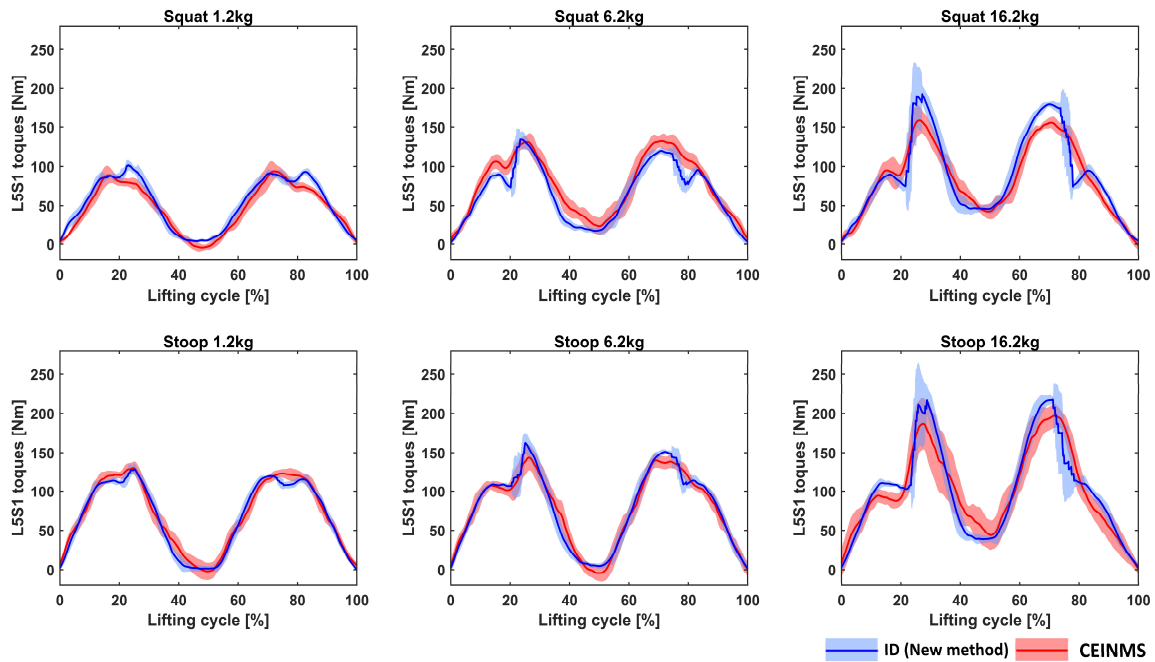


**Fig 9.** L5S1 torque estimates with new ID torques and CEINMS. Solid lines represent the average torques across repetitions and shaded areas correspond to  $\pm 1$  standard deviation.

CEINMS also resulted in good correlation and similar RMSE values for models calibrated with ID torques obtained from the new method. **Fig 9**, represents the comparison between L5S1 torques predicted by CEINMS models that were calibrated for squat and stoop lifting with ID torques from the new method. The values of  $r^2$  and RMSE are reported in the first row of **Table VI**.

RMSE and  $r^2$  values between torques estimated by CEINMS calibrated with old ID and new ID torques are represented in **Table VII**. The torque difference between both models for each trial is presented in **Fig 10**. The highest difference in torque was observed for Stoop 16.2kg (15.93 Nm).

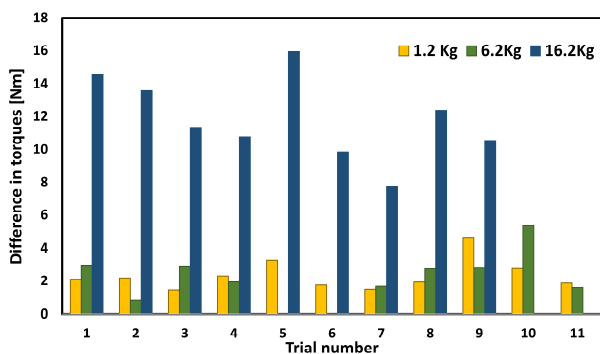


**Fig 10.** Difference between L5-S1 torques estimations of CEINMS calibrated with Old and new ID for stoop lifting

**TABLE VII**  
R2 AND RMSE VALUES FOR L5S1 TORQUES BETWEEN CEINMS calibrated with OLD ID AND CEINMS calibrated with NEW ID

	Squat 1.2kg	Squat 6.2kg	Squat 16.2kg	Stoop 1.2kg	Stoop 6.2kg	Stoop 16.2kg
$r^2$	0.99	0.99	0.99	0.99	0.99	0.99
RMS	0.84	0.80	1.11	2.33	2.34	3.21

#### D. Asymmetrical Lifting

For all asymmetric lifting trials, L5-S1 flexion-extension (F-E), axial rotation (AXR) and the lateral bending (LAT) ID torques estimated with old method and new methods can be seen in **Fig 11**. For LT, 0-20% of the trial corresponds to the instance at which the subject bent forward to pickup the box from the ground. The lift off instance can be seen around 15% of the trial marked by a sudden increase in the F-E torque for medium and higher weight condition ( 6.2 and 16.2 kg). The second peak observed for LT around 25-30% corresponds to transferring the load to the table placed on the right of the subject. This action was followed by returning back to upright position causing the F-E torques to decrease and become approximately 0 between 40-50% of the lifting cycle. The second half of the cycle, corresponds to picking up the box from the right and a lowering task to place the box to the ground between 90-100% of the trial. The AXR and LAT torques were observed to change during asymmetric movements (20-40% and 65-80%). The RMS and  $r^2$  values for comparison of old and new methods are reported in **Table VIII**. The highest RMS and lowest  $r^2$  were observed for axial rotation torques during 16.2 kg condition.

For TT tasks, 0-20% of the cycle represents twisting towards the left to pick up the box from the table and to transfer it on to a table on the right (20-30%). Twisting towards the left resulted in positive and negative LAT and AXR torques, respectively. This was followed by coming back to the upright position (30-40%) before beginning the second twist and transfer movement to return the box to it's original position. 60-100% of the cycle involved similar movements as 0-40% but with different medio-lateral direction (Z-axis). During this interval of the cycle, the subject picked up the box from the table on the right and moved it back to the table placed on the left of the

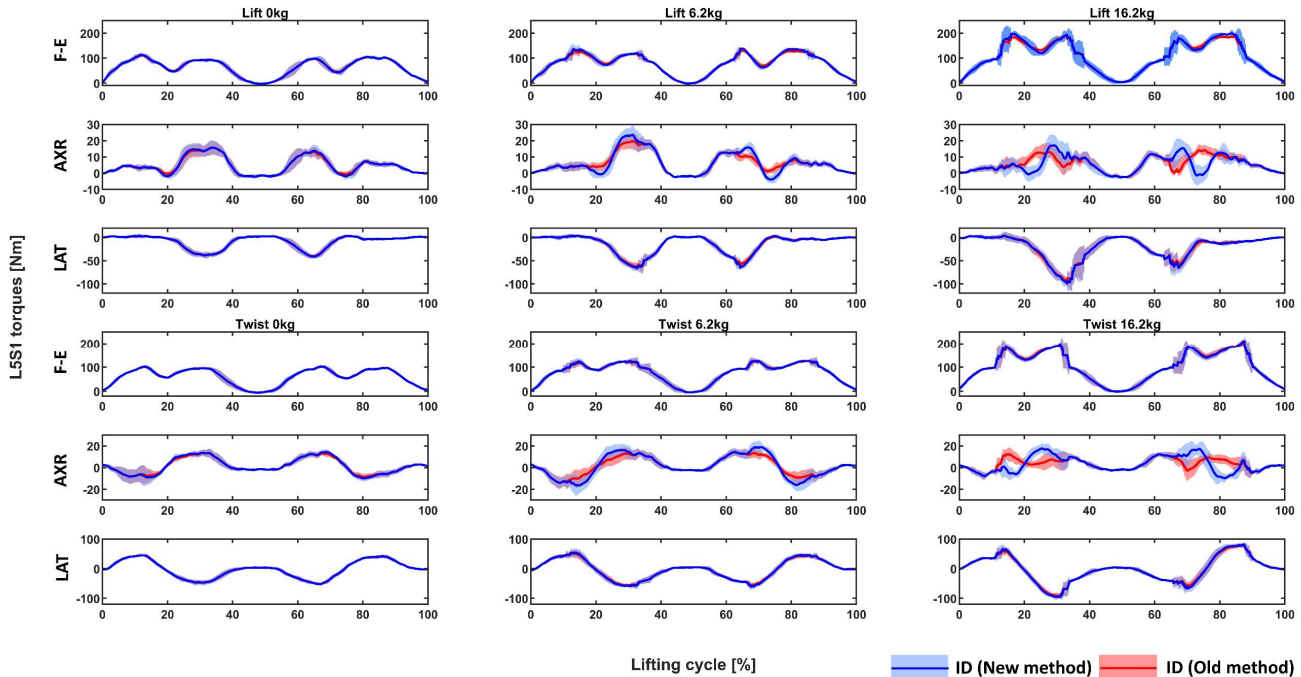


**Fig 11.** L5-S1 ID torque estimates with old and new method. Solid lines represent the average torques across repetitions and shaded areas correspond to  $\pm 1$  standard deviation. Note: F-E: Flexion-Extension, AXR: Axial rotation, LAT-Lateral bending L5-S1 torques.

TABLE VIII  
R2 AND RMSE VALUES FOR L5S1 TORQUES BETWEEN OLD AND NEW ID FOR ASYMMETRICAL TASKS

L-S1	LT 1.2 Kg		LT 6.2 Kg		LT 16.2 Kg		TT 1.2Kg		TT 6.2Kg		TT 16.2Kg	
	$r^2$	RMS	$r^2$	RMS	$r^2$	RMS	$r^2$	RMS	$r^2$	RMS	$r^2$	RMS
F-E	0.99	0.59	0.99	3.24	0.99	5.09	0.99	0.27	0.99	0.96	0.99	1.81
AXR	0.99	0.45	0.92	2.04	0.27	4.68	0.99	0.60	0.94	3.02	0.16	6.88
LAT	0.99	0.18	0.99	1.23	0.99	1.51	0.99	0.20	0.99	1.23	0.99	2.05

Note: F-E: Flexion-Extension, AXR: Axial rotation, LAT-Lateral bending torques, LT-Lift and transfer, TT-Twist and transfer

subject at  $60^\circ$ . L5-S1 torque for one repetition of each AL task is presented and explained in detail in **Appendix F**.

#### IV. DISCUSSION

The main goal of this study was to develop a novel methodology to accurately account for the inertial properties of the box during lifting tasks and to compute L5-S1 joint torques via EMG-driven modelling. Our proposed methodology consisted of modelling the kinetics of the box as an individual OpenSim model. Hence, allowing us to model tridimensional accelerations and rotational torques resulting from the box being lifted. Before the proposed methodology was implemented, several other approaches to account for hand forces from external objects were tested and are explained in Appendix C.

The method consisting of adding a box to the LFB model using weld joints described in Appendix C.1, could not be accomplished due to the closed-loop constraint in OpenSim, as it does not support bodies to be defined by two-parent frames (joint origin). The weld constraint model described in Appendix C.2 created additional constraints to the LFB model increasing the computational complexity during IK computations. This technique also resulted in unrealistic kinematics for pelvis, knee and feet with large errors for the IK solutions up to 18 cm. The IK

tool had also failed at instances when the set error tolerance of the order of  $10^{-6}$  was not achieved. We hypothesize that the reason behind the IK failure was that the box was held at different locations and orientations during each repetition, while the weld constraint assumed a fixed position and orientation between the hand and the box for all the repetitions. Due to this assumption, the experimental marker positions of the hands could not be tracked accurately for all trials. IK tool in OpenSim computes an optimal IK solution at each frame by reducing marker errors of all body markers with help of the least square estimation method [26]. Therefore, an error in the hand or box marker would indirectly result in errors for other markers in the model resulting in unrealistic kinematics.

The free joint approach presented in Appendix C.3 resulted in realistic kinematics for all the lifting tasks that were studied. However, estimations of L5-S1 torques during ID computations were erroneous. Erroneous torques could be explained by considering the inertial frame of the OpenSim model. The Pelvic frame of the base OpenSim model (LFB) is attached to the ground frame, therefore when an additional body was attached with a free joint to the ground frame, the translations of this body (box) during lifting tasks applied loads with moment arms to the pelvis and thus resulted in erroneous torques during ID computations. To evaluate the L5-S1 torques obtained with

the old method, the computed L5-S1 torques with the old method were compared to other studies that tested squat and stoop lifting for similar weight range. The obtained torques were in comparable range with other studies [7,36,41]. For all the symmetric trials, stoop lifting always resulted in higher L5-S1 torques when compared to the same weight lifted with squat lifting technique as seen in **Table V**. This is in accordance to the literature, where Abdoli-E et.al [41] compared stoop and squat lifting techniques and reported that stoop lifting resulted in higher L5-S1 torques [41]. Since the torques estimated with the old method were in par with other studies, the obtained torque estimates could be used as the baseline torques to study the new methodology.

Our proposed methodology of modelling the kinetics of the box as an individual OpenSim model resulted in increased L5-S1 peak torques for both squat and stoop lifting tasks, compared to ID torques derived from the old method. We hypothesize the reason behind such an increase is due to improved sensitivity of the new approach to account for forces due to tridimensional accelerations along with the rotational torques from the object. The old methodology proposed by Esteban et al.[36] on the other hand, only included a constant hand force based on the acceleration due to gravity in the vertical direction. However, for dynamic lifting tasks the user has to apply a net positive force to bring the object into acceleration and therefore hand forces would be higher than the weight of the object due to during gravity.

This hypothesis could be further bolstered with a closer inspection of standard deviations reported in **Table V**. The values indicate higher standard deviations for peak FE torques estimated with the new method when compared to the old method for all the lifting conditions. This suggests that the new method is more sensitive to the variability in lifting movements as it also accounted for acceleration during lifting, and orientation of the box while the old method indicated lower variability in the L5-S1 torques as it accounts only for acceleration due to gravity in the vertical direction and flexion-extension angles during movement. During the experimental sessions, the speed of the lifting tasks was not regulated, therefore this could have lead to higher accelerations of the box in a few trials. These differences, could not be captured by the old method as it did not account for accelerations of the box.

To test if the reported differences in L5-S1 torque estimates are statistically significant an ANOVA was conducted. The ANOVA indicated significant differences in L5-S1 (F-E) torques estimates between both methods. Other independent factors were also tested for significance to estimate L5-S1 (F-E) torque. Results indicated statistical significance for independent factors such as weight conditions and lifting techniques (stoop and squat). Kingma et.al. [6,7] also studied squat and stoop lifting tasks and reported significant effects for lifting techniques and lifting loads.

The proposed method was also tested for asymmetric lifting tasks. For LT tasks, L5-S1 (F-E) torques peaked around 20% of trial that involved lifting the box from the ground. The new methodology estimated higher L5-S1 (F-E) torques when compared to the old method for this interval of the lifting cycle as seen clearly in 6.2 and 16.2 kg weight condition in **Fig 11**. The L5-S1 torques (AXR and LAT) estimated with both methods were higher for 16.2 kg condition when compared to 1.2 kg for both methods. This suggested that although the transferring motion (asymmetry) was similar, the AXR and LAT torques are affected by the weight of the object being lifted. This effect was also reported by Kingma et al. in [42].

Although the new method increased the L5-S1 (F-E) torque estimates during lifting (20% of the cycle) of LT, the differences between the old and new method for transferring tasks were minimal. The differences between L5-S1 (F-E) torques estimates can be seen to be minimal during 30% and 70% of the lifting cycle for LT and 15% and 70% of the cycle for TT that correspond to transferring tasks. This could be explained by closely inspecting the kinematics of the box. During transferring tasks, the box was moved simultaneously in both mediolateral (Z-axis) and vertical (Y-axis) direction. Thus the forces from the box were divided over the two planes of lifting. This could be further confirmed by observing the LAT torques during the corresponding time interval of transferring tasks. The new method estimated higher LAT torques during transferring torques, this effect can be seen clearly for higher weight condition (16.2 kg) in **Fig 11** around 30 and 70% of the cycle when differences in F-E torques were minimal. When compared to LT, the TT tasks resulted in higher LAT and AXR torques by both methods. This suggests that the twisting movements cause higher LAT and AXR torques. Kim et al [6] also reported the increased effect of twisting movements on the L5-S1 LAT and L5-S1 AXR torques.

For higher weight condition (16.2 kg), L5-S1 AXR torques showed higher RMSE and lower correlation ( $r^2$ ) between both ID methods for TT tasks as seen in **Table VIII**. This could be explained by analyzing the differences between the hand forces that were applied during ID computations for both methods. The new methodology resulted in mediolateral shear hand forces (in Z-axis) of magnitude -20N during twisting movement, while the old methodology assumed 0 N force during movements in the mediolateral plane (Z-axis) as seen in Appendix F. Neglecting shear mediolateral hand forces from the box may have resulted in the erroneous estimation of axial rotation torques by the old ID method. Thus we assume that this hand force observed in the Z-axis (see Appendix F) caused the differences in L5-S1 (AXR) torque estimates between both methods during transferring tasks.

To check the sensitivity of CEINMS towards the new ID torques, CEINMS was calibrated with both new and old ID torques. CEINMS torques for models calibrated with both new ID and Old ID torques indicated good correlations and

low RMSE with respective reference ID torques. The RMSE for the squat lifting model was higher when compared to stoop lifting technique (19.69 Nm and 21.85 Nm for the model with old ID and new ID respectively) as seen in **Table VI**. The observed differences could have arisen from incorrect ID or CEINMS computations. The ID estimates could be improved by accurate scaling of the generic model to match the subject's anthropometric properties by using imaging techniques [36]. The errors in CEINMS estimates could be a result of suboptimal calibrations. The models were calibrated with just one repetition of an arbitrarily chosen dynamic trial for each weight condition. The calibrations could be improved by including more trials that include both static and dynamic lifting trials until the errors between the CEINMS torques estimates and ID estimates is minimized [35]. CEINMS models could also be calibrated for individual weight conditions to obtain more accurate CEINMS torques estimates to closely match the reference ID torques, however, this may not be feasible when translated to practical applications such as back-support exoskeleton control in industrial scenarios. CEINMS torques from model calibrated for new and old ID were compared to analyze the sensitivity of CEINMS to detect changes in ID torques from the new methodology. The results of the histograms in **Fig 10** indicated that CEINMS torques calibrated for new ID are higher (7.7-15.9 Nm) when compared CEINMS torques for a model calibrated with old ID. This indicated that our EMG-driven model is sensitive to differences in ID torques estimated with the new methodology.

By observing the improvements in L5-S1 torque estimations with the new method during both AL and SL tasks, we can say that our proposed method offers more realistic estimations of external hand forces and torques. Application of this methodology is not only limited to this specific OpenSim model used in this study but can also be used in conjunction with any open-source OpenSim model. The methodology also opens up an opportunity to estimate hand forces from any type of object that could be designed using CAD software such as SolidWorks.

Despite the improvement in the estimation of L5-S1 torques with our proposed methodology, there are few limitations that we would like to address regarding the design of the experiments. All the trials involved two repetitions of lifting cycles completed in 20s, however, the speed of lifting was not controlled. This resulted in different stages of the lifting not synchronized at the same percentage of the lifting cycle across repetitions. The effect of unsynchronized trials can be seen by observing the irregular standard deviations **Fig 6, 8, 9** and **11** especially during lift-off and drop off of the box. Future studies could use acoustic signals such as metronome to regulate the speed of lifting and synchronize different phases of lifting with % of lifting cycle across all repetitions. This can help in minimizing the variability between each repetition (SD) reported in **Table V**. Another limitation of this research is that the lifting instance of the box was detected based on

the vertical displacements of the box markers to apply hand forces. This could be improved by the use of external systems such as an external switch placed on the box to detect the lift-off [7]. EMG signals recorded from the hands could also be used to detect a change in muscle activation during the lift-off and drop off of the box. Including automatic detection of the time instance would allow modelling time instances between initial contact with the box and lift off.

## V. CONCLUSION

This research has successfully proposed an indirect methodology to improve modelling of external objects in OpenSim. The proposed approach has been tested for several types of lifting tasks including both symmetrical and asymmetrical lifting tasks and for a wide range of weight conditions relevant to the manual material handling industries. Results indicated statistically significant improvements in estimating peak L5-S1 torques for symmetric and asymmetrical lifting tasks, as it accounts for tri-dimensional accelerations and rotational torques of the box. The proposed methodology also increased CEINMS L5-S1(F-E) torque estimates. We believe that our proposed methodology can help in studying the etiology of lower back pain and could serve as a base for developing real-time back support exoskeleton controllers based on estimates of lumbar torques and compressive forces. We envision that this methodology could also be applied to all open-source OpenSim models to estimate external forces from any type of object to compute joint torques and compressive forces.

## REFERENCES

1. S. Madinei, M. M. Alemi, S. Kim, D. Srinivasan, and M. A. Nussbaum, "Biomechanical assessment of two back-support exoskeletons in symmetric and asymmetric repetitive lifting with moderate postural demands," *Applied Ergonomics*, vol. 88, pp. 103-156, 2020.
2. S. Toxiri, M. B. Näf, M. Lazzaroni, J. Fernández, M. Sposito, T. Poliero, L. Monica, S. Anastasi, D. G. Caldwell, and J. Ortiz, "Back-Support Exoskeletons for Occupational Use: An Overview of Technological Advances and Trends," *IIEE Transactions on Occupational Ergonomics and Human Factors*, vol. 7, no. 3-4, pp. 237-249, 2019.
3. L. Punnett, L. J. Fine, W. Keyserling, G. Herrin, and D. Chaffin, "Back disorders and nonneutral trunk postures of automobile assembly workers.," *Scandinavian Journal of Work, Environment & Health*, vol. 17, no. 5, pp. 337-346, 1991.
4. T. Zhang and H. Huang, "A Lower-Back Robotic Exoskeleton: Industrial Handling Augmentation Used to Provide Spinal Support," *IEEE Robotics & Automation Magazine*, vol. 25, no. 2, pp. 95-106, 2018.
5. Kingma, J. H. V. Dieën, M. D. Looze, H. M. Toussaint, P. Dolan, and C. T. Baten, "Asymmetric low back loading in asymmetric lifting movements is not prevented by pelvic twist," *Journal of Biomechanics*, vol. 31, no. 6, pp. 527-534, 1998.
6. H.-K. Kim and Y. Zhang, "Estimation of lumbar spinal loading and trunk muscle forces during asymmetric lifting tasks: application of whole-body musculoskeletal modelling in OpenSim," *Ergonomics*, vol. 60, no. 4, pp. 563-576, 2016.
7. Kingma, C. T. Baten, P. Dolan, H. M. Toussaint, J. H. V. Dieën, M. P. D. Looze, and M. A. Adams, "Lumbar loading during lifting: a comparative study of three measurement techniques," *Journal of Electromyography and Kinesiology*, vol. 11, no. 5, pp. 337-345, 2001.

8. H. K. Ko, S. W. Lee, D. H. Koo, I. Lee, and D. J. Hyun, "Waist-assistive exoskeleton powered by a singular actuation mechanism for prevention of back-injury," *Robotics and Autonomous Systems*, vol. 107, pp. 1–9, 2018.
9. S. Toxiri, "Rationale, Implementation and Evaluation of Assistive Strategies for an Active Back-Support Exoskeleton," *Bionics and Biomimetics*, May 2018.
10. 2020. *Manual Handling At Work A Brief Guide*. 4th ed. London, p.4.
11. M. P. D. Looze, T. Bosch, F. Krause, K. S. Stadler, and L. W. O'Sullivan, "Exoskeletons for industrial application and their potential effects on physical work load," *Ergonomics*, vol. 59, no. 5, pp. 671–681, 2015.
12. S. Toyama, "Wearable agrirobot," *JOURNAL OF VIBROENGINEERING*, vol. 12, no. 3, pp. 287–291, Sep. 2010.
13. M. Tsuzura, T. Nakakuki, and D. Misaki, "A mechanism design of waist power assist suit for a caregiver by using torsion springs," *2013 13th International Conference on Control, Automation and Systems (ICCAS 2013)*, 2013.
14. J. Naito, G. Obinata, A. Nakayama, and K. Hase, "Development of a Wearable Robot for Assisting Carpentry Workers," *Proceedings of the 23rd International Symposium on Automation and Robotics in Construction*, 2006.
15. H. Kazerooni, J.-L. Racine, L. Huang and R. Steger, On the control of the berkeley lower extremity exoskeleton (BLEEX), in *Proceedings of the 2005 IEEE International Conference on Robotics and Automation (ICRA)*, 2005
16. M. Sartori, M. Reggiani, D. Farina, and D. G. Lloyd, "EMG-Driven Forward-Dynamic Estimation of Muscle Force and Joint Moment about Multiple Degrees of Freedom in the Human Lower Extremity," *PLoS ONE*, vol. 7, no. 12, 2012.
17. Y. Imamura, T. Tanaka, Y. Suzuki, K. Takizawa, and M. Yamanaka, "Motion-based design of elastic belts for passive assistive device using musculoskeletal model," *2011 IEEE International Conference on Robotics and Biomimetics*, 2011.
18. E. P. Lamers, A. J. Yang, and K. E. Zelik, "Feasibility of a Biomechanically-Assistive Garment to Reduce Low Back Loading During Leaning and Lifting," *IEEE Transactions on Biomedical Engineering*, vol. 65, no. 8, pp. 1674–1680, 2018.
19. M. M. Alemi, J. Geissinger, A. A. Simon, S. E. Chang, and A. T. Asbeck, "A passive exoskeleton reduces peak and mean EMG during symmetric and asymmetric lifting," *Journal of Electromyography and Kinesiology*, vol. 47, pp. 25–34, 2019.
20. T. Bosch, J. V. Eck, K. Knitel, and M. D. Looze, "The effects of a passive exoskeleton on muscle activity, discomfort and endurance time in forward bending work," *Applied Ergonomics*, vol. 54, pp. 212–217, 2016.
21. K. Huysamen, M. D. Looze, T. Bosch, J. Ortiz, S. Toxiri, and L. W. O'Sullivan, "Assessment of an active industrial exoskeleton to aid dynamic lifting and lowering manual handling tasks," *Applied Ergonomics*, vol. 68, pp. 125–131, 2018.
22. Tucker, M. R., Olivier, J., Pagel, A., Bleuler, H., Bouri, M., Lambercy, O., Gassert, R. (2015). Control strategies for active lower extremity prosthetics and orthotics: A review. *Journal of NeuroEngineering and Rehabilitation*, 12(1), 1. doi:10.1186/1743-0003-12-1
23. Hara, H., & Sankai, Y. (2010). Development of HAL for lumbar support. Paper presented at SCIS and ISIS 2010—Joint 5th International Conference on Soft Computing and Intelligent Systems and 11th International Symposium on Advanced Intelligent Systems (pp. 416–421). SCIS & ISIS 2010, Dec. 8–12, 2010, Okayama Convention Center, Okayama, Japan Development.
24. Y. Blache, L. Desmoulin, P. Allard, A. Plamondon, and M. Begon, "Effects of height and load weight on shoulder muscle work during overhead lifting task," *Ergonomics*, vol. 58, no. 5, pp. 748–761, 2014.
25. F. Moissenet, L. Modenese, and R. Dumas, "Alterations of musculoskeletal models for a more accurate estimation of lower limb joint contact forces during normal gait: A systematic review," *Journal of Biomechanics*, vol. 63, pp. 8–20, 2017.
26. S. L. Delp *et al.*, "OpenSim: Open-Source Software to Create and Analyze Dynamic Simulations of Movement," in *IEEE Transactions on Biomedical Engineering*, vol. 54, no. 11, pp. 1940–1950, Nov. 2007, doi: 10.1109/TBME.2007.901024.
27. Seth, M. Sherman, J. A. Reinbolt, and S. L. Delp, "OpenSim: a musculoskeletal modeling and simulation framework for in silico investigations and exchange," *Procedia IUTAM*, vol. 2, pp. 212–232, 2011.
28. J. Fernandez and M. Pandy, "Integrating modelling and experiments to assess dynamic musculoskeletal function in humans", *Experimental physiology*, vol. 91, no. 2, pp. 371–382, 2006.
29. S. L. Delp, F. C. Anderson, A. S. Arnold, P. Loan, A. Habib, C. T. John, E. Guendelman, and D. G. Thelen, "Opensim: Open-source software to create and analyze dynamic simulations of movement", *IEEE transactions on biomedical engineering*, vol. 54, no. 11, pp. 1940–1950, 2007.
30. M. Damsgaard, J. Rasmussen, S. T. Christensen, E. Surma, and M. De Zee, "Analysis of musculoskeletal systems in the anybody modeling system", *Simulation Modelling Practice and Theory*, vol. 14, no. 8, pp. 1100–1111, 2006.
31. E. Beaucage-Gauvreau, W. S. P. Robertson, S. C. E. Brandon, R. Fraser, B. J. C. Freeman, R. B. Graham, D. Thewlis, and C. F. Jones, "Validation of an OpenSim full-body model with detailed lumbar spine for estimating lower lumbar spine loads during symmetric and asymmetric lifting tasks," *Computer Methods in Biomechanics and Biomedical Engineering*, vol. 22, no. 5, pp. 451–464, 2019.
32. T. S. Buchanan, D. G. Lloyd, K. Manal, and T. F. Besier, "Estimation of Muscle Forces and Joint Moments Using a Forward-Inverse Dynamics Model," *Medicine & Science in Sports & Exercise*, vol. 37, no. 11, pp. 1911–1916, 2005.
33. D. G. Lloyd and T. F. Besier, "An EMG-driven musculoskeletal model to estimate muscle forces and knee joint moments in vivo," *Journal of Biomechanics*, vol. 36, no. 6, pp. 765–776, 2003.
34. C. Pizzolato, D. G. Lloyd, M. Sartori, E. Ceseracciu, T. F. Besier, B. J. Fregly, and M. Reggiani, "CEINMS: A toolbox to investigate the influence of different neural control solutions on the prediction of muscle excitation and joint moments during dynamic motor tasks," *Journal of Biomechanics*, vol. 48, no. 14, pp. 3929–3936, 2015.
35. M. Sartori, M. Reggiani, D. Farina, and D. G. Lloyd, "EMG-Driven Forward-Dynamic Estimation of Muscle Force and Joint Moment about Multiple Degrees of Freedom in the Human Lower Extremity," *PLoS ONE*, vol. 7, no. 12, 2012.
36. A. Moya-Esteban, N. P. Brouwer, A. Tabasi, H. v. d. Kooij, I. Kingma and M. Sartori, "Muscle-level analysis of trunk mechanics via musculoskeletal modeling and high-density electromyograms," *2020 8th IEEE RAS/EMBS International Conference for Biomedical Robotics and Biomechanics (BioRob)*, New York City, NY, USA, 2020, pp. 1109–1114
37. Y. Blache, L. Desmoulin, P. Allard, A. Plamondon, and M. Begon, "Effects of height and load weight on shoulder muscle work during overhead lifting task," *Ergonomics*, vol. 58, no. 5, pp. 748–761, 2014.
38. E. Beaucage-Gauvreau, "Brace for it: assessing lumbar spinal loads for a braced arm-to-thigh lifting and bending technique using a musculoskeletal modelling approach," thesis, Research Theses, Adelaide, 2019
39. Kingma, G. S. Faber, A. J. Bakker, and Dieën Jaap H Van, "Can Low Back Loading During Lifting Be Reduced by Placing One Leg Beside the Object to Be Lifted?," *Physical Therapy*, vol. 86, no. 8, pp. 1091–1105, 2006.
40. A. Mantoan, C. Pizzolato, M. Sartori, Z. Sawacha, C. Cobelli, and M. Reggiani, "MotoNMS: A MATLAB toolbox to process motion data for neuromusculoskeletal modeling and simulation," *Source Code for Biology and Medicine*, vol. 10, no. 1, 2015.
41. M. Abdoli-E, M. J. Agnew, and J. M. Stevenson, "An on-body personal lift augmentation device (PLAD) reduces EMG amplitude of erector spinae during lifting tasks," *Clinical Biomechanics*, vol. 21, no. 5, pp. 456–465, 2006.
42. Kingma, J. H. V. Dieën, M. D. Looze, H. M. Toussaint, P. Dolan, and C. T. Baten, "Asymmetric low back loading in asymmetric lifting movements is not prevented by pelvic twist," *Journal of Biomechanics*, vol. 31, no. 6, pp. 527–534, 1998.

## APPENDIX

## A. Conventions of OpenSim

The coordinate conventions followed by OpenSim is shown in **Fig A1**. Green vertical line defines the Y-axis, the blue line represents the Z-axis and X-axis is represented by the red line.

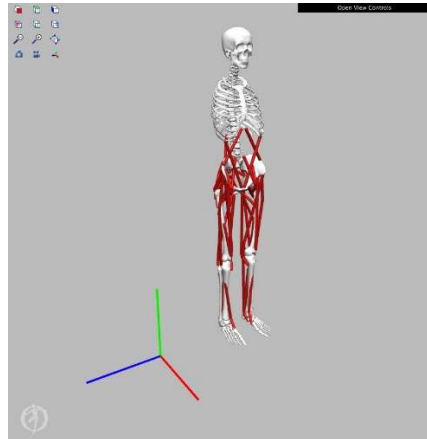


**Fig A1.** Co-ordinate convention OpenSim

## B. Creating Box model in Solidworks

The designs were created in the same coordinate conventions as the OpenSim model. The files were exported in .stl file format. The following export settings options were used

- Checked do not translate STL data into positive space
- Default export settings (binary output, Meters units, default output coordinate system) were used

The box of dimensions 40 cm x 30 cm x 20cm (width x depth x height) had a volume of  $0.0264 \text{ m}^3$ . The density of 1.2, 6.2 and 16.2kg was calculated to be 45.454, 234.848 and  $613.636 \text{ kgm}^{-3}$  respectively. The origin of the box was defined at the mass centre. The moments of inertia were obtained from SolidWorks. The set mass and density properties along with the resultant moment of inertia can be seen in **Fig B1, B2 and B3**.

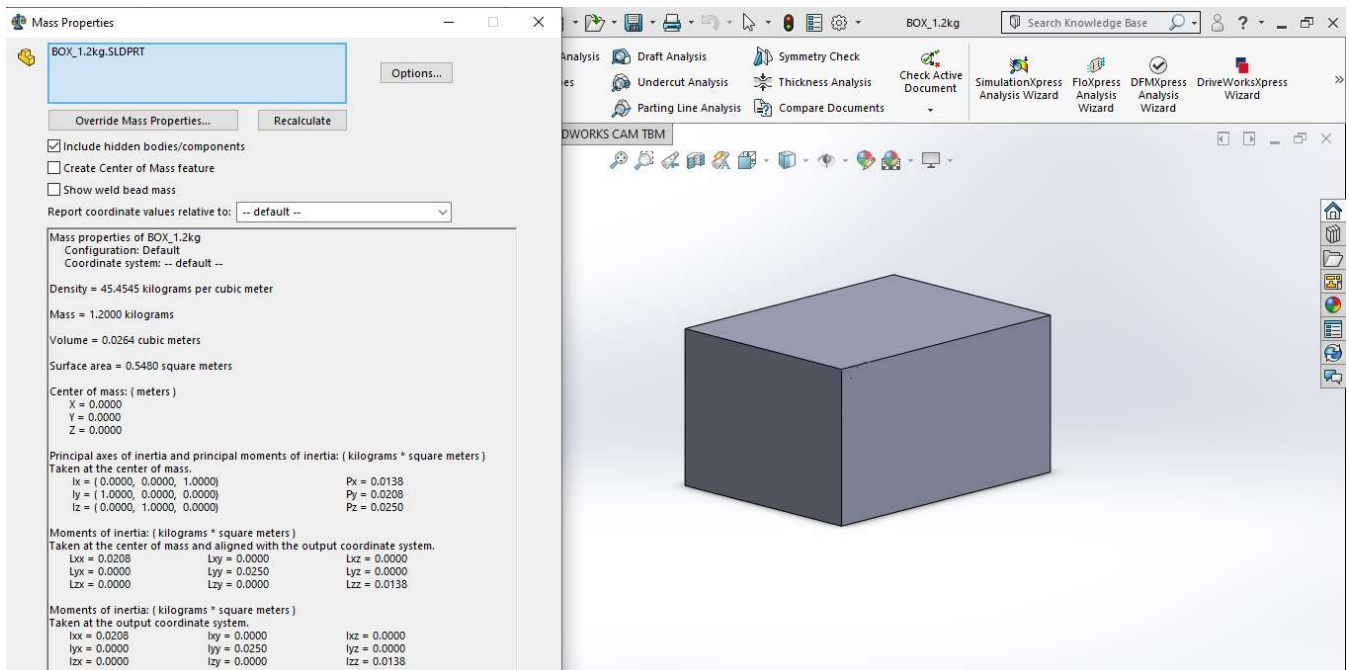


**Fig B1.** Box mass and inertial properties 1.2kg

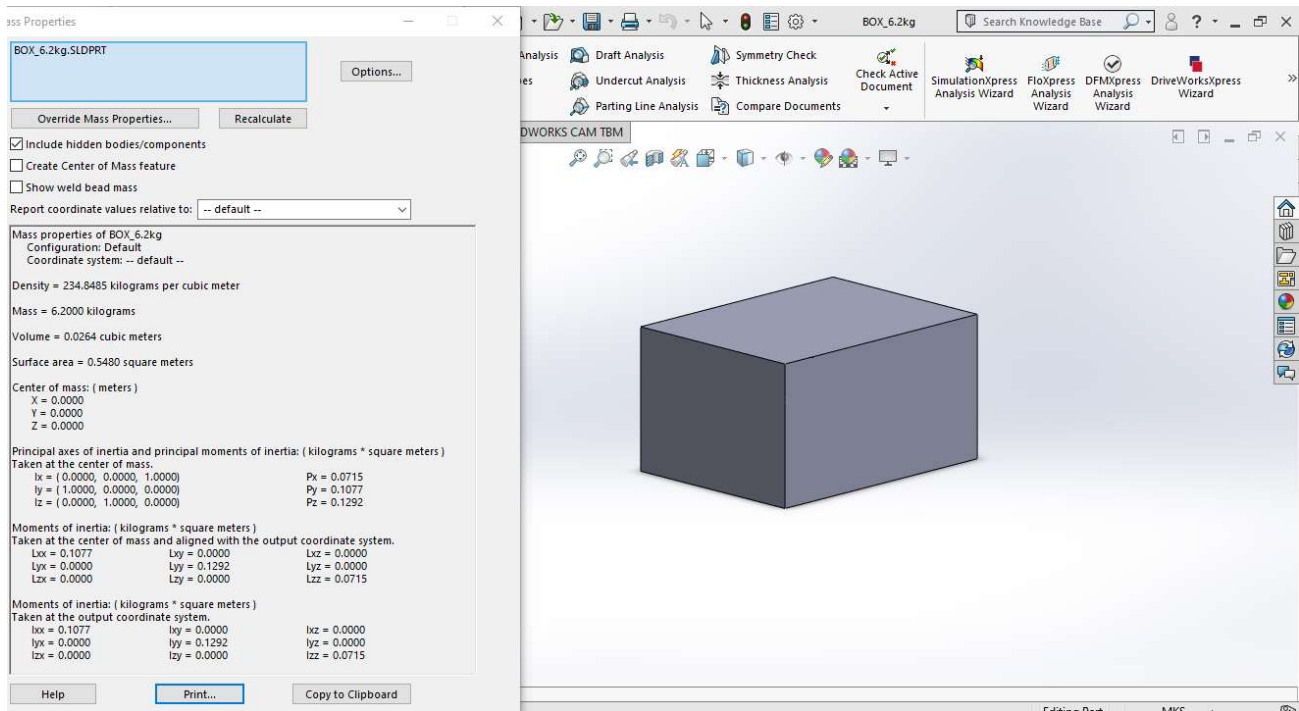


Fig B2. Box mass and inertial properties 6.2kg

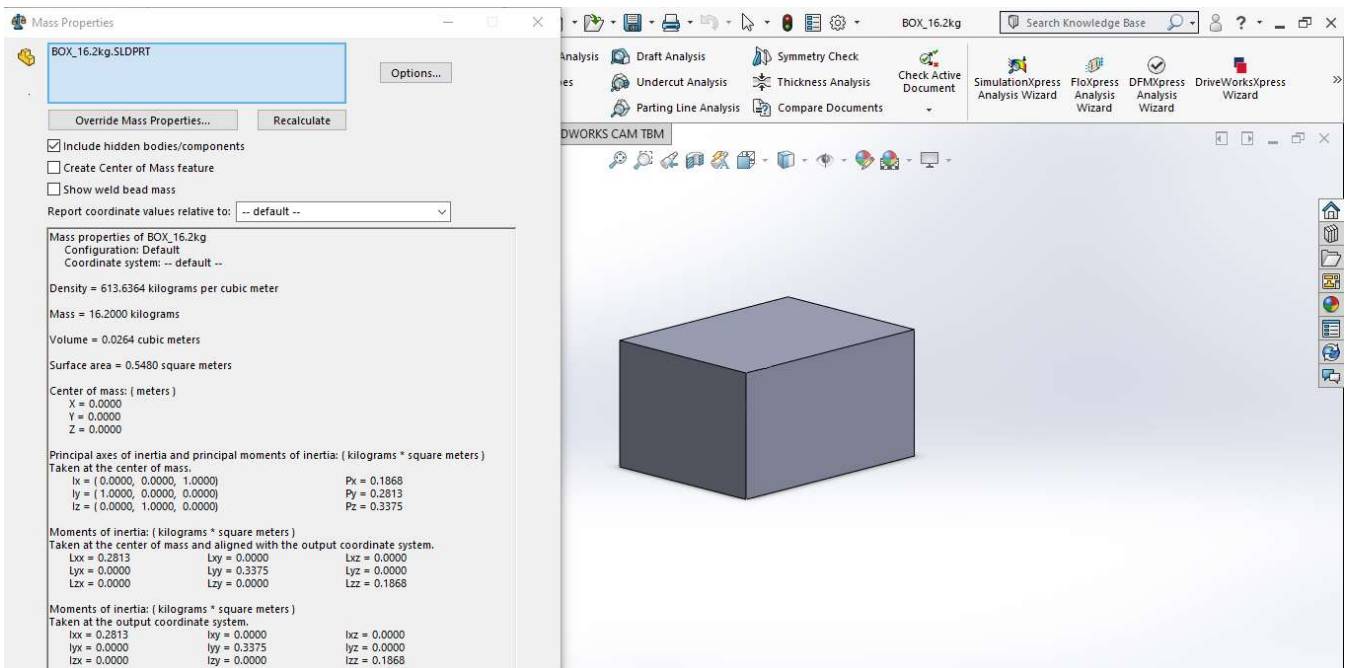


Fig B3. Box mass and inertial properties 16.2kg

### C. Adding the box to OpenSim model

#### 1) Box with a weld joint

A weld joint between the box and each hand was created based on the assumptions of Balche et al. A weld joint produces 0 DOF connections between the objects and fuses them [1]. Every joint in the OpenSim model, consists of child frame and a parent frame to which the child is attached. The weld joint between the right hand and the box was defined by keeping the hand and box as parent and child frame respectively. The weld joint between the box and left hand was defined by assuming the box to be the parent of the left hand. This method created a closed kinematic loop constraint in OpenSim and thus could not be implemented.

#### 2) Box with a weld constraint

One of the weld joints explained in the previous subsection C.1 was converted into a weld constraint. Weld constraints create a constraint between the box and the hand to align the coordinate frames of both the bodies during motion [1]. A weld joint was created between the right hand and the box while the box was defined as a parent to the left hand for the weld constraint.

Therefore, the left hand would follow the coordinate frames of the box. One disadvantage of this method is that it assumes that the box is always attached to the hands. Therefore, only the time frames at which the box was in contact with the hands during the trial could be modelled. IK for the time instances at which the box was in the hands was performed in OpenSim. Several iterations of adjusting weights of leg and box markers were also tested. ID computations were performed with only the GRF forces and moments.

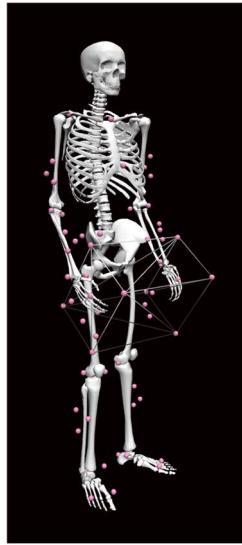


Fig C1. LFB model with box added as a weld constraint

### 3) Box with a free joint

A free joint was implemented between the box and the ground. A free joint adds the box to the LFB model and allows 3 translations and 3 rotational movements. Translational offsets were defined between the ground and the box to replicate the initial position at which the box was placed before the beginning of each trial. IK and ID were performed for both symmetrical lifting techniques for the entire trial. The results of the models are discussed in section IV of the paper.

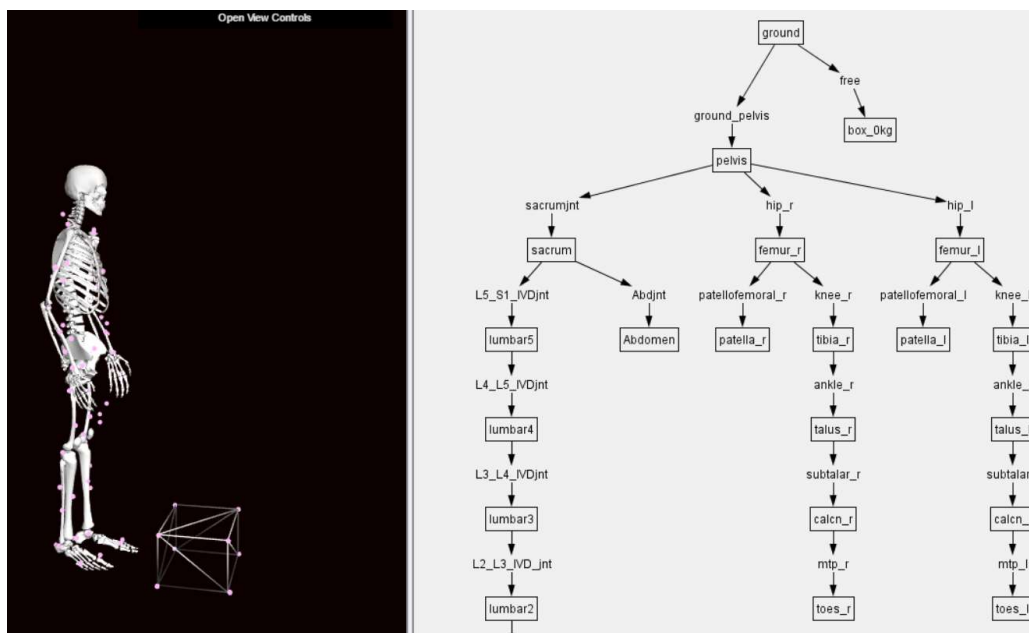


Fig C2. LFB model with box added as a free joint

### D. Symmetrical lifting tasks

Fig D.1 represents L5-S1(F-E) torques for squat lifting tasks. It can be seen that there is an increase in L5-S1 torque estimates between both methods for the interval at which the hand forces are applied. The increase could be explained with help of the hand forces. The initial negative peak observed in the new hand force is a result of a positive force applied by the subject on to the box to lift the box from the ground. The hand force is seen to decrease and become less negative as the subject holding the box decelerates to back to an upright position with the box. The change in L5-S1 torque between both methods was also observed during lowering activity when the subject moves to return the box to its original position. A similar difference between both methods was also observed for stoop lifting.



Fig D.1. L5-S1(F-E) torques for Squat 16.2 kg condition

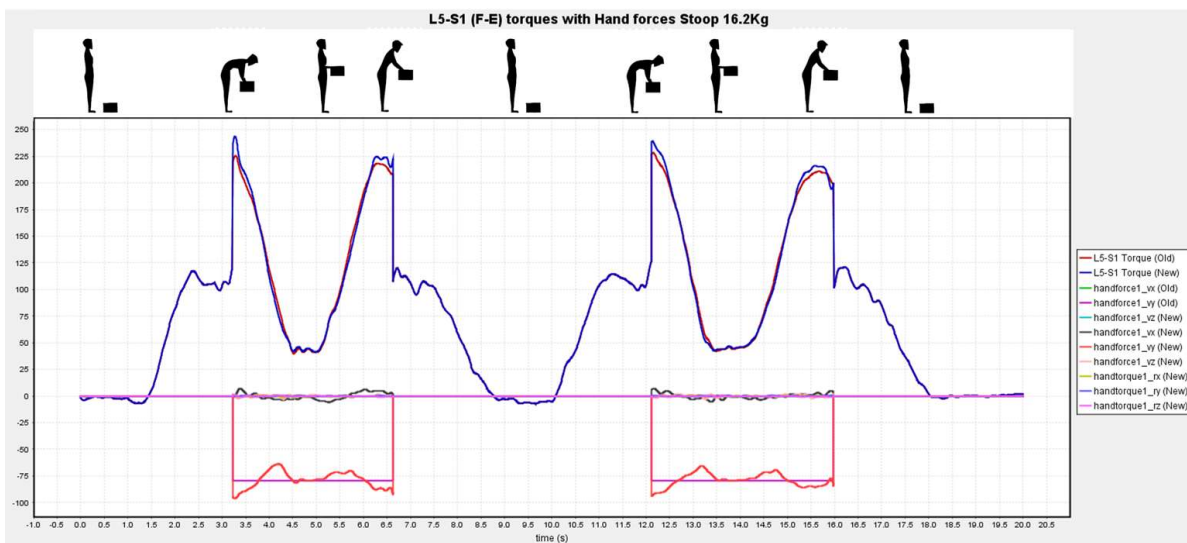


Fig D.2. L5-S1(F-E) torques for Stoop 16.2 kg condition

### E. ANOVA for symmetric lifting tasks

Results of ANOVA for symmetric lifting trials can be seen in Table. The L5-S1(F-E) torques were considered to be the dependent variable. Factors such as weight of the box, lifting method (stoop or squat), estimation method (new ID or old ID method) were considered as independent factors. The effect of independent factors along with their interaction effects on the dependent variable was studied using ANOVA with  $\alpha=0.05$ .

**Tests of Between-Subjects Effects**

Dependent Variable: Torques

Source	Type III Sum of Squares	df	Mean Square	F	Sig.
Corrected Model	267704.465 <sup>a</sup>	11	24336.770	686.191	.000
Intercept	3818955.687	1	3818955.687	107677.963	.000
Weight	224320.791	2	112160.395	3162.436	.000
Estimation_method	3117.609	1	3117.609	87.903	.000
Lifting_method	37782.485	1	37782.485	1065.302	.000
Weight* Estimation_method	1330.959	2	665.480	18.764	.000
Weight* Lifting_method	775.832	2	387.916	10.938	.000
Estimation_method* Lifting_method	195.758	1	195.758	5.520	.020
Weight* Estimation_method* Lifting_method	181.031	2	90.516	2.552	.082
Error	4681.572	132	35.466		
Total	4091341.725	144			
Corrected Total	272386.037	143			

a. R Squared = .983 (Adjusted R Squared = .981)

Fig E.1. Results of ANOVA performed in SPSS

### F. Asymmetrical Lifting tasks

One trial with two repetitions of TL task is shown in **Fig F.1**. The blue solid square represents the lifting task. The subject deployed free lifting technique to pick up the box. The box was lifted in the mid- sagittal plane. The lifting was similar to squat lifting. The Flexion extension torques estimated by the new method was higher than the old method. The blue dashed box represents the transferring task. During this motion, the difference between both methods was minimal. Transferring task involved simultaneous lifting the box in both Y and X direction. This can be seen in the Ik results of the box in **Fig F.2**. During the transferring movement, although the new method resulted in higher F-E torques, it increased LAT torque at the same instance of the blue dotted box. The AXR torques represented in black solid lines also follow the hand force\_vz represented by a yellow solid line. We can also see the difference between AXR torque between old and new methods ( green and yellow) in **Fig F.1**.

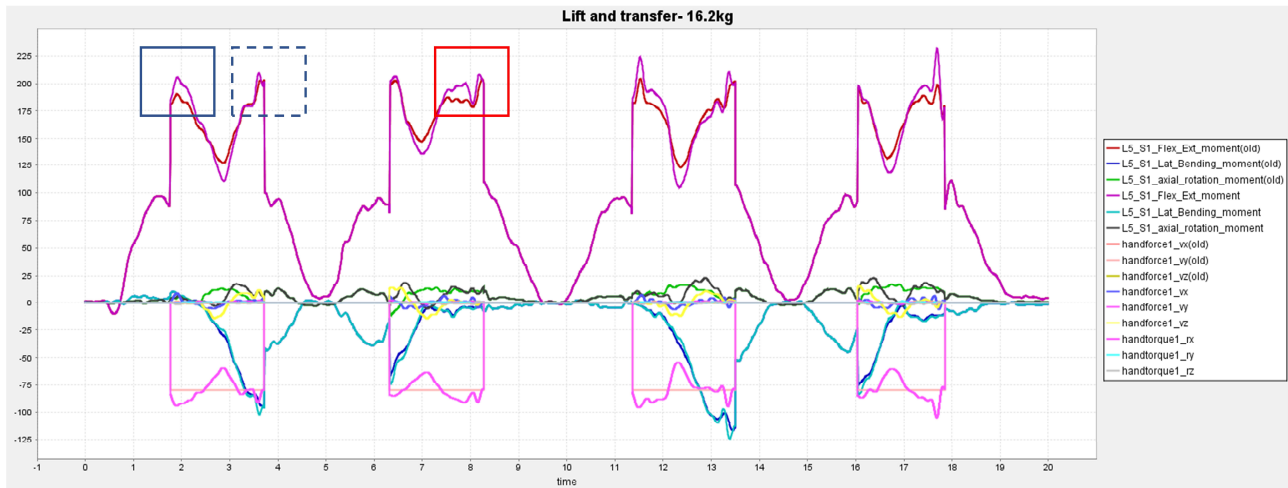


**Fig F.1.** L5-S1 torques for Lift and transfer 16.2 kg condition

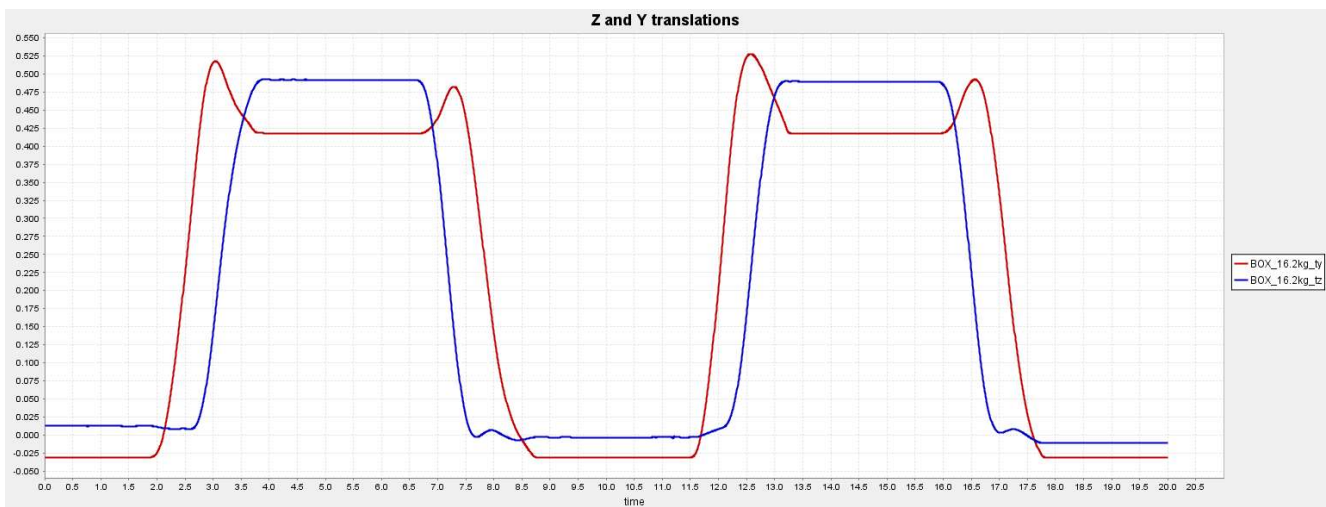


**Fig F.2.** Z and Y translation of the box during Lift and transfer task (16.2 kg condition)

One trial of Twist and transfer with 16.2 kg condition is seen in **Fig F.3**. The AXR torque from the old method (green) and the new method (black) appeared different from each other. The new AXR torques resemble the handforce\_Vz during transferring tasks. The new handforce\_vz can be seen to have a magnitude of -20 to 20N when compared to old handforce\_vz of 0N. We assume that this force acts in the z-axis to create an axial rotation torque in the lumbar spine. However, in the old method, the observed AXR torque was only due to the twisting movement of the lumbar spine.

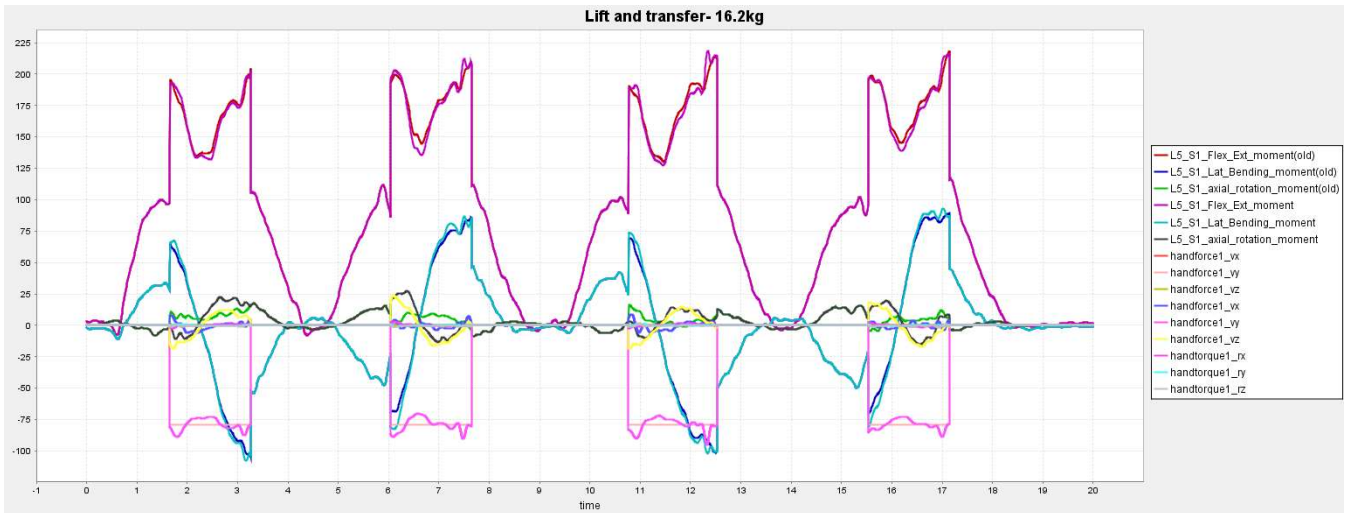


Fig F.3. L5-S1 torques for Lift and transfer 16.2 kg condition

#### REFERENCES ( Appendix)

1. "OpenSim Documentation - OpenSim Models," *OpenSim Documentation - OpenSim Documentation - Global Site*. [Online]. Available: <https://simtk-confluence.stanford.edu:8443/display/OpenSim>. [Accessed: 07-Oct-2020].